Stable singularity-free cosmological solutions in nonprojectable Hořava-Lifshitz gravity

Mitsuhiro Fukushima,* Yosuke Misonoh,† Shoichiro Miyashita,‡ and Seiga Sato§
Department of Physics, Waseda University, Okubo 3-4-1, Shinjuku, Tokyo 169-8555, Japan

(Received 3 January 2019; published 6 March 2019)

We find stable singularity-free cosmological solutions in nonflat Friedmann-Lemaître-Robertson-Walker (FLRW) spacetime in the context of Hořava-Lifshitz (HL) theory. Although we encounter the negative squared effective masses of the scalar perturbations in the original HL theory, the behaviors can be remedied by relaxing the projectability condition. In our analysis, the effects from the background dynamics are taken into account as well as the sign of the coefficients in the quadratic action for perturbations. More specifically, we give further classification of the gradient stability/instability into five types. These types are defined in terms of the effective squared masses of perturbations $\mathcal{M}^2$, the effective friction coefficients in perturbation equations $\mathcal{H}$ and these magnitude relations $|\mathcal{M}^2|/\mathcal{H}^2$. Furthermore, we indicate that oscillating solutions possibly show a kind of resonance especially in open FLRW spacetime. We find that the higher-order spatial curvature terms with Lifshitz scaling $z = 3$ are significant to suppress the instabilities due to the background dynamics.

DOI: 10.1103/PhysRevD.99.064004

I. INTRODUCTION

From the invention of big bang theory, resolving the cosmological initial singularity problem has been one of the most intriguing research frontiers in theoretical physics. According to the singularity theorem proved by Hawking and Penrose [1], a spacetime singularity must exist at a finite past of the big bang universe based on the general relativity (GR) unless some unnatural conditions are imposed. Even if the inflation which resolves the fine tuning problems in the very early stage of the Universe is introduced, the initial singularity cannot be remedied [2].

Since the initial singularity spoils the predictability at the beginning of the Universe, many researchers have been proposed cosmological scenarios to remove the singularity(see [3] for a review). For example, in the context of braneworld [4], string gas [5], loop quantum gravity [6–8], Horndeski theory (or generalized Galileon) [9–14], and the nonlocal gravitational theory [15]. In spite of these efforts, we have not achieved the completely stable singularity-free cosmological scenario, yet. Recently, striking studies have been conducted. A quite wide class of singularity-free cosmological solutions in Friedmann-Lemaître-Robertson-Walker (FLRW) spacetime is proved to be unstable [16–19]. Since the no-go theorem is established based on the Horndeski theory, in other words, the most generalized scalar-tensor theory whose equation of motion is up to second order [20], one may consider it is difficult to find stable cosmological solutions without a singularity. However, certain loopholes of the no-go theorem are known [21–25]. One example of such loophole is to consider a Lorenz violating gravitational theory. The no-go theorem is possibly violated by introducing higher-order spatial derivative terms [22].

Hořava-Lifshitz (HL) theory is known as a gravitational theory without Lorentz symmetry, which is a candidate for quantum gravity [26] (the recent progresses of the HL theory are reviewed in [27]). As we have known, the spin-2 gravitational field cannot be quantized in perturbative approach, that is, there is infinite number of loop diagrams with ultraviolet divergence. In contrast, the HL theory realizes renormalizability at least at power-counting level by introducing the Lifshitz scaling,

$$t \to b^{-z}t \quad \text{and} \quad x^i \to b^{-1}x^i, \tag{1.1}$$

which is an anisotropic scaling between time t and space x^i. A dynamical critical exponent z characterizes a degree of anisotropy. If z is equal to or greater than the spatial dimension, ultraviolet divergence can be suppressed by finite number of counter terms [26,28,29].

In the context of the HL theory, a number of attractive applications for cosmology have been conducted (see [30] for a review): for example, primordial perturbations [31–35], gravitational waves [36,37] and other cosmological aspects [38–41]. It is remarkable that the bouncing and oscillating solutions are discovered as singularity-free cosmological models in HL theory [42–47]. Lifshitz scaling terms up to $z = 3$ which realizes the power-counting

*m.fukushima@aoni.waseda.jp
†y_misonou@moegi.waseda.jp
‡miyashita@gravity.phys.waseda.ac.jp
§s.seiga@gravity.phys.waseda.ac.jp

renormalizability in four-dimensional spacetime derive squared and cubed three-dimensional Ricci curvatures in the action. These terms behave as radiationlike and stiff matterlike components in nonflat FLRW spacetime. As we will mention, these components can effectively violate the energy condition, which is one of the postulates in the singularity theorem.

In our previous paper [48], we investigated the stability of the singularity-free cosmological solutions based on the projectable HL theory. Namely, we impose following the projectability condition:

$$N(t, x^i) \to N(t), \tag{1.2}$$

where N is the lapse function which is one of the Arnowitt-Deser-Misner (ADM) variables. It turns out that the HL theory with the projectability condition suffers from the instability when the effects of higher-order curvature terms are irrelevant [49–52]. More specifically, we encounter the negative squared effective masses of scalar perturbations in FLRW spacetime. To suppress the instability, we must consider a strong Hubble friction by introducing a positive cosmological constant.

In fact, the pathological behavior in infrared region is possibly remedied by considering a theory without the projectability condition, that is the nonprojectable HL theory [53]. It is discovered that the gradient instability in flat FLRW spacetime can be avoided [54,55]. Therefore, it is expected that the infrared instabilities of the singularity-free solutions in nonflat FLRW spacetime are improved.

Although the nonprojectable HL theory possesses the attractive feature [27,56–63], the most general form of the gravitational action is extremely complicated. Since what we would like to clarify is to examine whether the nonprojectable HL theory can improve the infrared behavior after singularity avoidance or not, we will focus only on an additional term which is dominant in infrared regime, which is the minimally extended HL action.

The rest of this paper is organized as follows. In Sec. II, we construct the nonprojectable HL action with the minimal extension from the projectable one. The background dynamics in nonflat FLRW spacetime and the classification of the singularity-free solutions are reviewed in Sec. III. In Sec. IV, we perform the perturbative analysis by deriving the quadratic action. The decomposition of the perturbation modes and the manner of the gauge fixing are also summarized. Then, in Sec. V, we discuss the stability of singularity-free solutions in nonflat FLRW spacetime. We give further classification of the gradient stability/instability into five types to consider the background effects. Sec. VI is devoted to summary and discussions.

II. MINIMALLY EXTENDED NONPROJECTABLE HOŘAVA-LIFSHITZ THEORY

As we mentioned, Lifshitz scaling with $z > 1$ induces the anisotropy between space and time, which means the general covariance in four-dimensional spacetime is no longer valid. We instead find a fundamental symmetry called foliation-preserving diffeomorphism:

$$t \to t + f(t), \qquad x^i \to x^i + \zeta^i(t, x^j), \tag{2.1}$$

namely, a boost transformation is prohibited. Thus, it is clearly preferable to adopt the ADM quantities, the three-dimensional spatial metric g_{ij}, the lapse function N and the shift vector N^i as the fundamental variables. In order to preserve the invariance under (2.1), the terms in action must be composed of the following quantities: The extrinsic curvature which is defined by

$$\mathcal{K}_{ij} \coloneqq \frac{1}{2N}(\dot{g}_{ij} - \nabla_i N_j - \nabla_i N_j), \tag{2.2}$$

where the *dot* symbol represents the derivative with respect to time coordinate and ∇_i denotes the spatial covariant derivative. The three dimensional Ricci curvature $\mathcal{R}_{ij}$ associated with the spatial covariant derivative. Since we relax the projectability condition, the spatial dependence of the lapse function is restored. Thus, the following vector quantity can be included in the action:

$$\Phi_i \coloneqq \frac{\nabla_i N}{N}, \tag{2.3}$$

which represents the acceleration of rest observer on three-dimensional hypersurface. Furthermore, spatial covariant derivatives of these quantities also form the invariant action, i.e., $\nabla_i\mathcal{K}_{jk}$, $\nabla_i\mathcal{R}_{jk}$, $\nabla_i\Phi_j$, $\nabla_i\nabla_j\mathcal{K}_{kl}$ and so on.

Although we can include every scalar quantities which are composed of these variables to construct the invariant action, our model is restricted as follows:

$$S = \frac{m_{\rm LV}^2}{2}\int dt\, d^3x(\mathcal{L}_{\rm K} + \mathcal{L}_{\rm P} + \mathcal{L}_{\rm NP}), \tag{2.4}$$

with

$$\mathcal{L}_{\rm K} \coloneqq N\sqrt{g}(\mathcal{K}_{ij}\mathcal{K}^{ij} - \lambda\mathcal{K}^2), \tag{2.5}$$

$$\mathcal{L}_{\rm P} \coloneqq -N\sqrt{g}[\mathcal{V}_{z=1} + m_{\rm LV}^{-2}\mathcal{V}_{z=2} + m_{\rm LV}^{-4}\mathcal{V}_{z=3}], \tag{2.6}$$

$$\mathcal{L}_{\rm NP} \coloneqq N\sqrt{g}\mathcal{V}[\Phi_i], \tag{2.7}$$

$$\begin{aligned}
\mathcal{V}_{z=1} &\coloneqq 2\Lambda + g_1\mathcal{R},\\
\mathcal{V}_{z=2} &\coloneqq g_2\mathcal{R}^2 + g_3\mathcal{R}^i{}_j\mathcal{R}^j{}_i,\\
\mathcal{V}_{z=3} &\coloneqq g_4\mathcal{R}^3 + g_5\mathcal{R}\mathcal{R}^i{}_j\mathcal{R}^j{}_i + g_6\mathcal{R}^i{}_j\mathcal{R}^j{}_k\mathcal{R}^k{}_i\\
&\quad + g_7\mathcal{R}\nabla^2\mathcal{R} + g_8\nabla_i\mathcal{R}_{jk}\nabla^i\mathcal{R}^{jk},
\end{aligned} \tag{2.8}$$

where $m_{\rm LV}$ is a Lorentz violating scale which is expected to be around the Planck scale, λ and g_i $(i = 1\text{–}8)$ are

dimension-less coupling constants and Λ is a cosmological constant. $\mathcal{L}_{\rm NP}$ is constructed by the terms including Φ_i field, which is with no effect to FLRW background. The reason for the restriction is to ensure the comparability of our previous result based on the SVW action [64]. As we will see in the next section, the background dynamics are identical to those of the SVW action under specific condition.

We further impose a restriction on $\mathcal{L}_{\rm NP}$. Recall that the purpose of this paper is to remedy the infrared behavior of bouncing solutions discovered in the projectable HL theory. It is naturally expected that the terms with the lowest order of spatial derivative is essential to stabilize the infrared region. In fact, such a term is uniquely determined, that is $\Phi^2 \coloneqq \Phi_i\Phi^i$. According to the papers [53], the stabilities of Minkowski and flat FLRW spacetime are remedied by the nonprojectable HL theory with Φ^2 term. Therefore, we do minimally extend the theory by adding only Φ^2 term:

$$\mathcal{V}[\Phi_i] \coloneqq \varsigma\Phi^2. \tag{2.9}$$

with a dimensionless coupling constant ς.

In the rest of this paper, the unit $m_{\rm LV} = 1$ is adopted. We additionally can set the value of the coupling constant by rescaling the time coordinate. Thus, we set $g_1 = -1$, which is equivalent to take a coordinate in which the propagating speed of the spin-2 gravitational wave in infrared limit is precisely unity [37,65].

III. BACKGROUND SOLUTIONS IN FLRW SPACETIME

The Hamiltonian constraint in the nonprojectable HL theory is quite different from the projectable one. In other words, the Hamiltonian constraint is defined at each spacetime point. In this section, we briefly summarize the structure of the basic equation system and the classification of singularity-free solutions in FLRW spacetime.

A. Basic equations

To unify the description, we consider the FLRW spacetime in a spatial coordinate system $x^i = (\chi, \theta, \phi)$:

$$\begin{aligned} ds^2 &= g_{ij}dx^i dx^j \\ &= a^2[d\chi^2 + f(\chi)^2(d\theta^2 + \sin^2\theta d\phi^2)], \end{aligned} \tag{3.1}$$

with

$$f(\chi) \coloneqq \begin{cases} \chi & \text{for } K = 0 \\ \sin\chi & \text{for } K = 1 \\ \sinh\chi & \text{for } K = -1 \end{cases}, \tag{3.2}$$

where a is the scale factor which depends only on the cosmic time, and K is related to the spatial Ricci curvature as $\mathcal{R} = 6K/a^2$. The cases with $K = 0, 1$ and -1 correspond to the flat, closed and open FLRW spacetime, respectively. The domain of the coordinate χ is defined by $0 \le \chi < \infty$ for $K = 0, -1$ and $0 \le \chi \le \pi$ for $K = 1$. Furthermore, angular coordinates θ and ϕ take $0 \le \theta \le \pi$ and $0 \le \phi \le 2\pi$, respectively.

Then, the dynamical equation for the scale factor and the Friedmann equation are obtained by taking variation of the action with respect to a and N:

$$2\dot{H} + 3H^2 = \frac{2}{3\lambda - 1}\left(\Lambda - \frac{K}{a^2} - \frac{g_r K^2}{3a^4} - \frac{g_s K^3}{a^6}\right), \tag{3.3}$$

$$H^2 = \frac{2}{3(3\lambda - 1)}\left[\Lambda - 3\frac{K}{a^2} + \frac{g_r K^2}{a^4} + \frac{g_s K^3}{a^6}\right], \tag{3.4}$$

where $H \coloneqq \dot{a}/a$ is the Hubble parameter, g_r and g_s are the linear combinations of the coupling constants[1]:

$$g_r \coloneqq 6(3g_2 + g_3), \tag{3.5}$$

$$g_s \coloneqq 12(9g_4 + 3g_5 + g_6). \tag{3.6}$$

We have already fixed the gauge as $N = 1$ and $N_i = 0$. In what follows, we assume $\lambda > 1/3$.

As we know, the equation of the scale factor (3.3) can be derived by taking derivative of (3.4) with respect to the cosmic time. It means the independent equation is only (3.4). However, the situation with the projectability condition is quite different. Due to the lack of the local lapse function, the Hamiltonian constraint is an integration over whole space. Therefore, we have to adopt the scale factor equation instead of the global Hamiltonian constraint in the projectable case. Friedmann-like equation is derived by integration with respect to the cosmic time:

$$H^2 = \frac{2}{3(3\lambda - 1)}\left[\Lambda - 3\frac{K}{a^2} + \frac{g_r K^2}{a^4} + \frac{g_s K^3}{a^6} + \frac{\mathcal{C}}{a^3}\right], \tag{3.7}$$

with dustlike term with an integration constant $\mathcal{C}$ [39]. Thus, if we consider $\mathcal{C} = 0$ case in the projectable HL theory, the same background FLRW solutions are realized [46,48].

B. Singularity-free background solutions

In order to investigate the background solutions, it is convenient to rewrite the Friedmann equation (3.4) into

[1]It should be noted that we adopt the different definitions of g_r and g_s from our previous paper [48] to simplify the perturbed action. The previous definitions are

$$g_r \coloneqq 6K^2(3g_2 + g_3), \qquad g_s \coloneqq 12K^3(9g_4 + 3g_5 + g_6);$$

thus, the sign of g_s is flipped in open FLRW spacetime.

$$\frac{1}{2}\dot{a}^2 + \mathcal{U}(a) = 0, \tag{3.8}$$

with

$$\mathcal{U}(a) = \frac{1}{3\lambda - 1}\left[K - \frac{\Lambda}{3}a^2 - \frac{g_r K^2}{3a^2} - \frac{g_s K^3}{3a^4}\right]. \tag{3.9}$$

Since the possible ranges for the scale factor are limited within the region in which $\mathcal{U} \leq 0$, the background evolution is completely determined by the coupling constants in $\mathcal{L}_{\rm P}$. It is remarkable that the g_r and the g_s terms simulate a radiation component and a stiff matter component, respectively. The important point is that these terms can effectively violate the energy condition if either or both of $g_r K^2$ and $g_s K^3$ are negative, which may lead singularity-free solutions even if we do not introduce some exotic matters.

The classification of the possible solutions is given in Ref. [46]. In our analysis, we focus on the following two kinds of singularity-free solutions. One is a bouncing solution denoted by $\mathcal{B}^{[\mathrm{sgn}(\Lambda);K]}$, where the function $\mathrm{sgn}(x)$ gives a sign of x. An initial contracting universe shifts to expanding phase at $a = a_T$ and keep expanding forever. The other is oscillating solution denoted by $\mathcal{O}^{[\mathrm{sgn}(\Lambda);K]}$. A universe shows periodic oscillating behavior, in other words, bounces at $a = a_{\rm min}$ and recollapses[2] at $a = a_{\rm max}$. Therefore, the scale factor is limited within $0 < a_{\rm min} \leq a \leq a_{\rm max} < \infty$. As we will see, the typical size of the oscillating amplitude is expected to be the Lorentz violating scale, thus, it is difficult to represent the cyclic universe scenario whose maximum scale factor is macroscopic.

1. Without cosmological constant

In our previous paper [48], we have found that the stable singularity-free solutions require a positive cosmological constant based on the projectable HL theory. Once the projectability condition is relaxed, it is expected to find stable bouncing solutions without a cosmological constant as is the case in flat FLRW spacetime. Therefore, we summarize the singularity-free cosmological solutions without a cosmological constant in this part.

Since the sign of $\mathcal{U}$ determines the possible ranges for the scale factor, it is convenient to derive the roots of the equation $\mathcal{U} = 0$:

$$a_{\pm}^{[K]} = \sqrt{\frac{K}{6}\left(g_r \pm \sqrt{g_r^2 + 12 g_s}\right)}. \tag{3.10}$$

The points $a = a_{\pm}^{[K]}$ correspond to the bouncing or recollapsing points of the Universe. Of course, the corresponding $a_{\pm}^{[K]}$ must be real and positive to find such points. By examining the forms of the potential $\mathcal{U}$, we find the following three types of singularity-free solutions.

(a) $\mathcal{O}^{[0;1]}$—A universe shows oscillating behavior in closed FLRW spacetime ($K = 1$), which we call $\mathcal{O}^{[0;1]}$. This type of the solutions can be found if the following conditions are satisfied.

$$g_s < 0, g_r > 0 \quad \text{and} \quad g_r^2 + 12 g_s > 0$$
$$\text{with} \quad a_{\rm max} = a_{+}^{[1]} \quad \text{and} \quad a_{\rm min} = a_{-}^{[1]}.$$

In open FLRW spacetime, this kind of solutions is never found.

(b) $\mathcal{B}^{[0;-1]}$—An initially contracting universe shifts to expanding phase at bouncing point $a = a_T$, and keeps expanding forever in open FLRW spacetime ($K = -1$). This type of the solutions is classified into the following two cases:

(i) $\forall\, g_r$ and $g_s > 0$ with $a_T = a_{-}^{[-1]}$.
(ii) $g_r < 0$ and $g_s = 0$ with $a_T = a_{-}^{[-1]}$.

The solutions satisfying the conditions (i) and (ii) are referred to as $\mathcal{B}^{[0;-1]}$ (i) and $\mathcal{B}^{[0;-1]}$ (ii), respectively. In closed FLRW spacetime, we cannot find this type of the solutions.

(c) $\mathcal{B}_{\rm BC}^{[0;-1]}$—A universe shows bouncing behavior if the initial value of scale factor $a_{\rm ini}$ is larger than a_T, whereas it falls down into the singularity if $a_{\rm ini} \leq a_{\rm BC}$. Since this type of solution possibly induces a big crunch (BC), we add a subscript BC. Note that the domain $a_{\rm BC} < a < a_T$ is prohibited because the Hamiltonian constraint is never satisfied. If the following conditions are satisfied in open FLRW spacetime ($K = -1$), $\mathcal{B}_{\rm BC}^{[0;-1]}$ can be found:

$$g_s < 0, \quad g_r < 0 \quad \text{and} \quad g_r^2 + 12 g_s > 0$$
$$\text{with} \quad a_T = a_{-}^{[-1]} \quad \text{and} \quad a_{\rm BC} = a_{+}^{[-1]},$$

where $a_{\rm BC}$ is a recollapsing point of the big crunch universe. This type of bouncing solutions is found only in open FLRW spacetime.

We show the typical forms of potentials of $\mathcal{O}^{[0,1]}$, $\mathcal{B}^{[0,-1]}$ and $\mathcal{B}_{\rm BC}^{[0,-1]}$ in Fig. 1 and the distribution of these types of solutions on the (g_r, g_s) plane in Fig. 2.

As we will discuss later, we can construct the bouncing solutions $\mathcal{B}^{[0;-1]}$ and $\mathcal{B}_{\rm BC}^{[0;-1]}$ whose squared effective masses of scalar perturbations are positive. Therefore, there is a possibility to construct stable singularity-free solutions without a cosmological constant. It is a striking difference from the projectable HL theory.

[2]In this paper, "recollapse" means that the expanding universe shifts to contracting phase. Thus, a recollapsing point satisfies the conditions $\mathcal{U} = 0$ and $\mathcal{U}' > 0$.

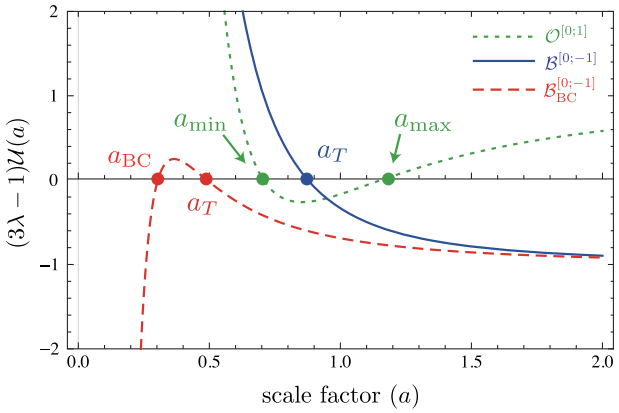

FIG. 1. The typical potential forms for singularity-free cosmological solutions without a cosmological constant. The dotted green, solid blue and dashed red curves indicate $\mathcal{O}^{[0;1]}$, $\mathcal{B}^{[0;-1]}$ and $\mathcal{B}^{[0;-1]}_{\rm BC}$, respectively. We set the coupling constants to $g_r = 11/2$ and $g_s = -2$ for $\mathcal{O}^{[0;1]}$, $g_r = -1$ and $g_s = 1$ for $\mathcal{B}^{[0;-1]}$, $g_r = -1$ and $g_s = -1/15$ for $\mathcal{B}^{[0;-1]}_{\rm BC}$.

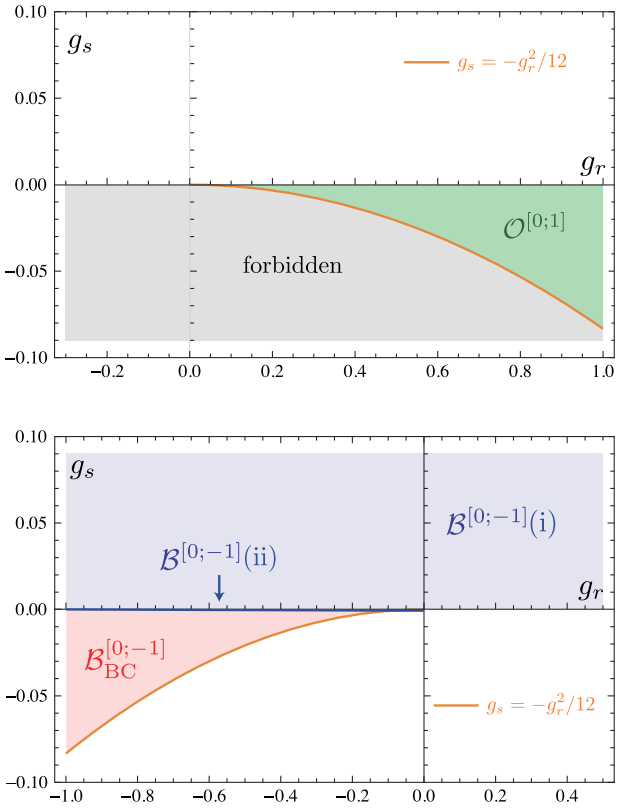

FIG. 2. The distribution of the singularity-free solutions for $\Lambda = 0$ in (g_r, g_s) plane. The top and bottom figures correspond to closed and open FLRW spacetime, respectively. The green, blue and red regions indicate the solutions of $\mathcal{O}^{[0;1]}$, $\mathcal{B}^{[0;-1]}$ (i) and $\mathcal{B}^{[0;-1]}_{\rm BC}$, respectively. $\mathcal{B}^{[0;-1]}$ (ii) is distributed on the blue line. The gray region is forbidden because the Hamiltonian constraint is never satisfied.

2. With positive cosmological constant

Although the properties of singularity-free solutions for $\Lambda > 0$ have already given in the papers [46,48], we again summarize the solutions because the notation is slightly changed from previous ones. When we consider the case with nonzero cosmological constant, it is convenient to introduce the following quantities normalized by a cosmological constant; $\tilde{a} := a/\ell$, $\tilde{g}_r := g_r/\ell^2$ and $\tilde{g}_s := g_s/\ell^4$ with $\ell := \sqrt{3/|\Lambda|}$. Then, the potential $\mathcal{U}$ is rewritten as

$$\tilde{\mathcal{U}}(\tilde{a}) = \frac{1}{3\lambda - 1}\left[K - \varepsilon\tilde{a}^2 - \frac{\tilde{g}_r K^2}{3\tilde{a}^2} - \frac{\tilde{g}_s K^3}{3\tilde{a}^4}\right], \tag{3.11}$$

where $\varepsilon := \pm 1$ expresses the sign of the cosmological constant. The three roots of the equation $\tilde{\mathcal{U}}(\tilde{a}) = 0$ are given by

$$\tilde{a}_I^{[\varepsilon;K]} := \sqrt{\frac{K}{6\varepsilon}\left[2 + \frac{4(1-\tilde{g}_r)}{\tilde{\xi}_I^{[\varepsilon;K]}} + \tilde{\xi}_I^{[\varepsilon;K]}\right]}, \tag{3.12}$$

with

$$\tilde{\xi}_I^{[\varepsilon;K]} := 2^{2/3}(e^{2\pi i/3})^I \,\mathrm{pv}\Big[2 - 3\varepsilon\tilde{g}_r - 9\tilde{g}_s + 9\mathrm{sgn}(K)\sqrt{\left(\tilde{g}_s - \tilde{g}_{s(+)}^{[\varepsilon;K]}\right)\left(\tilde{g}_s - \tilde{g}_{s(-)}^{[\varepsilon;K]}\right)}\Big]^{1/3}, \tag{3.13}$$

$$\tilde{g}_{s(\pm)}^{[\varepsilon;K]} := \frac{1}{9}[2 - 3\varepsilon\tilde{g}_r \pm 2\mathrm{sgn}(K)(1 - \varepsilon\tilde{g}_r)^{3/2}], \tag{3.14}$$

where pv means a principal value of cubic root and $I = 1, 2, 3$. If $\tilde{a}_I^{[\varepsilon;K]}$ takes real and positive value, $\tilde{\mathcal{U}}(\tilde{a}) = 0$ possesses a corresponding root in the possible ranges for the scale factor. We further derive the roots of $\tilde{\mathcal{U}}(\tilde{a}) = 0$ with $\tilde{g}_s = 0$:

$$\tilde{a}_\pm^{[\varepsilon;K]} := \sqrt{\frac{K}{2\varepsilon}\left[1 \pm \mathrm{sgn}(K)\sqrt{1 - \frac{4\varepsilon\tilde{g}_r}{3}}\right]}. \tag{3.15}$$

We classify the singularity-free solutions with a positive cosmological constant $(\varepsilon = +1)$ into the following three types:

(a) $\mathcal{B}^{[1;K]}$—A bouncing solution whose bouncing radius is given as $\tilde{a}_T$. We refer to this type of solution as $\mathcal{B}^{[1;K]}$. Unlike the case without a cosmological constant, the Universe after the bounce approaches de Sitter spacetime. For closed FLRW spacetime $(K = 1)$, we can find $\mathcal{B}^{[1;1]}$ as the following three cases:

(i) $\tilde{g}_{s(+)}^{[1;1]} < \tilde{g}_s < 0$ and $\tilde{g}_r < 1$ with $\tilde{a}_T = \tilde{a}_1^{[1;1]}$.

(ii) $\begin{cases} \tilde{g}_s < 0 \text{ and } \tilde{g}_s < \tilde{g}_{s(-)}^{[1;1]} & \text{for } |2\tilde{g}_r - 1| < 1 \\ \tilde{g}_s < 0 & \text{for } |2\tilde{g}_r - 1| \geq 1 \end{cases}$ with $\tilde{a}_T = \tilde{a}_3^{[1;1]}$.

(iii) $\tilde{g}_s = 0$ and $\tilde{g}_r \leq 0$ with $\tilde{a}_T = \tilde{a}_+^{[1;1]}$.

The solutions satisfying the conditions (i), (ii) and (iii) are referred to as $\mathcal{B}^{[1;1]}$ (i), $\mathcal{B}^{[1;1]}$ (ii) and $\mathcal{B}^{[1;1]}$ (iii), respectively. For open FLRW spacetime ($K=-1$), we find $\mathcal{B}^{[1;-1]}$ as the following two cases:

(i) $\tilde{g}_s > 0$ with $\tilde{a}_T = \tilde{a}_3^{[1;-1]}$.

(ii) $\tilde{g}_s = 0$ and $\tilde{g}_r < 0$ with $\tilde{a}_T = \tilde{a}_+^{[1;-1]}$.

$\mathcal{B}^{[1;-1]}$ (i) and $\mathcal{B}^{[1;-1]}$ (ii) correspond to the conditions (i) and (ii), respectively.

(b) $\mathcal{B}_{\rm BC}^{[1;K]}$—A universe with $\tilde{a}_{\rm ini} \le \tilde{a}_{\rm BC}$ evolves into a big crunch, while it shows bouncing behavior if $\tilde{a}_{\rm ini} \ge \tilde{a}_T > \tilde{a}_{\rm BC}$. We classify this type of solution as $\mathcal{B}_{\rm BC}^{[1;K]}$. Unlike $\mathcal{B}_{\rm BC}^{[0;K]}$, the asymptotic behavior of spacetime after bounce is de Sitter spacetime. For closed FLRW spacetime ($K=1$), we find the following two cases:

(i) $0 < \tilde{g}_s < \tilde{g}_{s(+)}^{[1;1]}$ with $\tilde{a}_{\rm BC} = \tilde{a}_2^{[1;1]}$ and $\tilde{a}_T = \tilde{a}_3^{[1;1]}$.

(ii) $\tilde{g}_s = 0$ and $0 < \tilde{g}_r < \frac{3}{4}$ with $\tilde{a}_{\rm BC} = \tilde{a}_-^{[1;1]}$ and $\tilde{a}_T = \tilde{a}_+^{[1;1]}$.

The solutions satisfying the conditions (i) and (ii) are referred to as $\mathcal{B}_{\rm BC}^{[1;1]}$ (i) and $\mathcal{B}_{\rm BC}^{[1;1]}$ (ii), respectively. For open FLRW spacetime ($K=-1$), the solutions $\mathcal{B}_{\rm BC}^{[1;-1]}$ can be seen when the following conditions are satisfied:

$0 > \tilde{g}_s > \tilde{g}_{s(+)}^{[1;-1]}$ and $\tilde{g}_r < 0$ with $\tilde{a}_{\rm BC} = \tilde{a}_2^{[1;-1]}$ and $\tilde{a}_T = \tilde{a}_3^{[1;-1]}$.

(c) $\mathcal{B}_O^{[1;1]}$—A universe in closed FLRW spacetime shows oscillating behavior if the initial scale factor is in $\tilde{a}_{\rm min} \le \tilde{a}_{\rm ini} \le \tilde{a}_{\rm max}$, or bounces if $\tilde{a}_{\rm ini} \ge \tilde{a}_T > \tilde{a}_{\rm max}$. We classify this type of solution as $\mathcal{B}_O^{[1;1]}$. The subscript represents the oscillating behavior. This type of solution can be found in closed FLRW spacetime ($K=1$) if the following conditions are satisfied.

$\tilde{g}_s < 0$ and $\tilde{g}_{s(-)}^{[1;1]} < \tilde{g}_s < \tilde{g}_{s(+)}^{[1;1]}$ with $\tilde{a}_{\rm min} = \tilde{a}_1^{[1;1]}$, $\tilde{a}_{\rm max} = \tilde{a}_2^{[1;1]}$ and $\tilde{a}_T = \tilde{a}_3^{[1;1]}$.

For open FLRW spacetime, we never find this type of solution.

The typical forms of potentials and the distribution of the singularity-free solutions on $(\tilde{g}_r, \tilde{g}_s)$ plane are shown in Figs. 3 and 4, respectively.

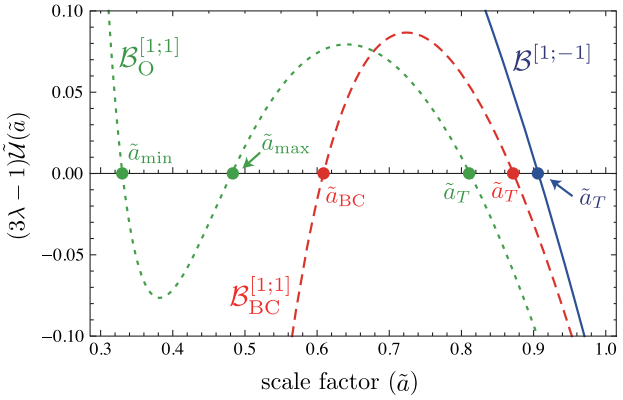

FIG. 3. The typical potential forms for singularity-free cosmological solutions with a positive cosmological constant. The solid blue, dashed red and dotted green curves indicate $\mathcal{B}^{[1;-1]}$, $\mathcal{B}_{\rm BC}^{[1;1]}$ and $\mathcal{B}_{\rm O}^{[1;1]}$, respectively. We set the coupling constants to $\tilde{g}_r = 1/2$ and $\tilde{g}_s = 1/20$ for $\mathcal{B}^{[1;-1]}$, $\tilde{g}_r = 2/5$ and $\tilde{g}_s = 1/9$ for $\mathcal{B}_{\rm BC}^{[1;1]}$, $\tilde{g}_r = 3/4$ and $\tilde{g}_s = -1/20$ for $\mathcal{B}_{\rm O}^{[1;1]}$.

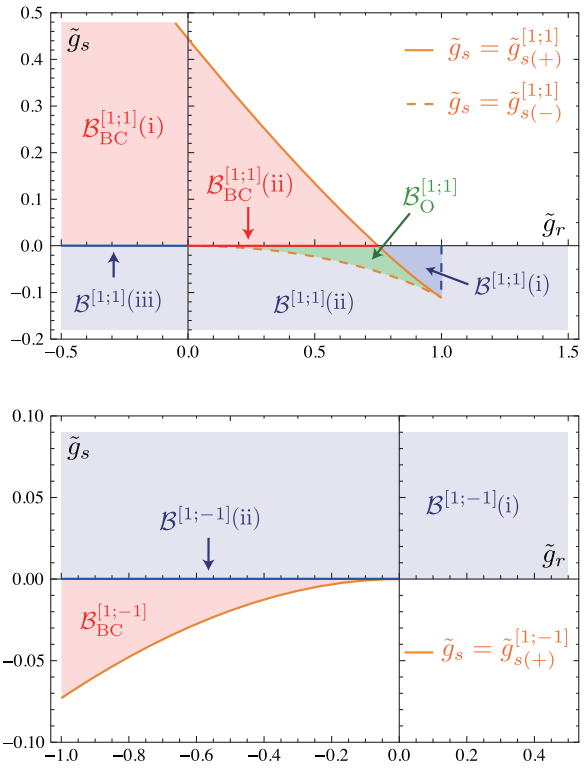

FIG. 4. The distribution of the singularity-free solutions for $\Lambda > 0$ in (g_r, g_s) plane. The top and bottom figures correspond to closed and open FLRW spacetime, respectively. The blue, red and green regions indicate the solutions of $\mathcal{B}^{[1;K]}$, $\mathcal{B}_{\rm BC}^{[1;K]}$ and $\mathcal{B}_{\rm O}^{[1;1]}$, respectively. $\mathcal{B}^{[1;1]}$ (iii), $\mathcal{B}^{[1;-1]}$ (ii) and $\mathcal{B}_{\rm BC}^{[1;1]}$ (ii) are located on the $\tilde{g}_s$ axis.

3. With negative cosmological constant

In this paper, we discuss the stabilities of the oscillating solutions as well as the bouncing solutions. Thus, we do not exclude the solutions with a negative cosmological constant ($\varepsilon = -1$), which we cannot construct the bouncing solutions. We find the following two kinds of singularity-free oscillating solutions:

(a) $\mathcal{O}^{[-1;K]}$—A universe which shows periodic oscillation whose oscillating amplitude is given by $\tilde{a}_{\rm min} \le \tilde{a} \le \tilde{a}_{\rm max}$. We classify this type of solution as $\mathcal{O}^{[-1;K]}$. If the following conditions are satisfied in closed FLRW spacetime ($K = 1$), $\mathcal{O}^{[-1;1]}$ is realized:

$$\tilde{g}^{[-1;1]}_{s(-)} < \tilde{g}_s < 0 \quad \text{with} \quad \tilde{a}_{\rm min} = \tilde{a}^{[-1;1]}_2 \quad \text{and} \quad \tilde{a}_{\rm max} = \tilde{a}^{[-1;1]}_1.$$

In open FLRW spacetime ($K = -1$), we find the two cases of $\mathcal{O}^{[-1;-1]}$ are obtained:

(i) $0 < \tilde{g}_s < \tilde{g}^{[-1;-1]}_{s(-)}$ with $\tilde{a}_{\rm min} = \tilde{a}^{[-1;-1]}_2$ and $\tilde{a}_{\rm max} = \tilde{a}^{[-1;-1]}_1$.

(ii) $\tilde{g}_s = 0$ and $-\frac{3}{4} < \tilde{g}_r < 0$ with $\tilde{a}_{\rm min} = \tilde{a}^{[-1;-1]}_+$ and $\tilde{a}_{\rm max} = \tilde{a}^{[-1;-1]}_-$.

The solutions satisfying the conditions (i) and (ii) are referred to as $\mathcal{O}^{[-1;-1]}$ (i) and $\mathcal{O}^{[-1;-1]}$ (ii), respectively.

(b) $\mathcal{O}^{[-1;-1]}_{\rm BC}$—A universe in open FLRW spacetime shows oscillating behavior if the initial radius of the Universe is in $\tilde{a}_{\rm min} \le \tilde{a}_{\rm ini} \le \tilde{a}_{\rm max}$, or falls into the singularity if $\tilde{a}_{\rm ini} < \tilde{a}_{\rm BC} < \tilde{a}_{\rm min}$. We refer to this type of solution as $\mathcal{O}^{[-1;-1]}_{\rm BC}$. For open FLRW spacetime ($K = -1$), we find the solutions under the following conditions:

$$\tilde{g}_s < 0 \quad \text{and} \quad \tilde{g}^{[-1;-1]}_{s(+)} < \tilde{g}_s < \tilde{g}^{[-1;-1]}_{s(-)} \quad \text{with} \quad \tilde{a}_{\rm BC} = \tilde{a}^{[-1;-1]}_3, \quad \tilde{a}_{\rm min} = \tilde{a}^{[-1;-1]}_2 \quad \text{and} \quad \tilde{a}_{\rm max} = \tilde{a}^{[-1;-1]}_1.$$

In closed FLRW spacetime, we cannot construct this type of solution.

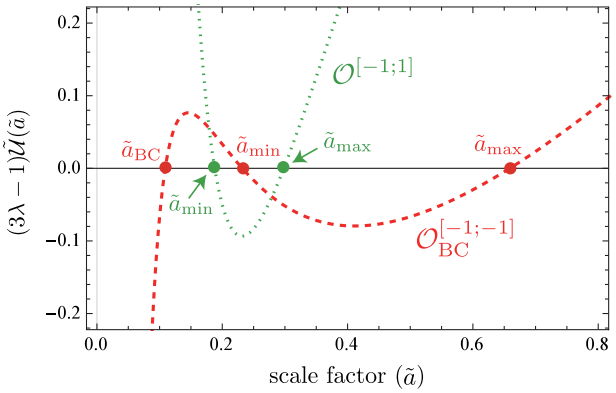

FIG. 5. The typical potential forms for singularity-free cosmological solutions with negative cosmological constants. The dotted green and dashed red curves indicate $\mathcal{O}^{[-1;1]}$ and $\mathcal{O}^{[-1;-1]}_{\rm BC}$, respectively. We set the coupling constants to $\tilde{g}_r = 2$ and $\tilde{g}_s = -1/4$ for $\mathcal{O}^{[-1;1]}$, $\tilde{g}_r = -3/4$ and $\tilde{g}_s = -1/20$ for $\mathcal{O}^{[-1;-1]}_{\rm BC}$.

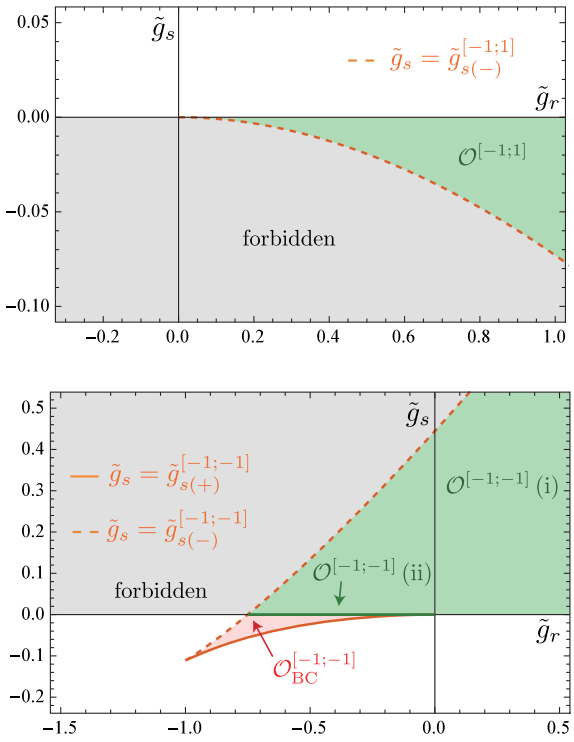

FIG. 6. The distribution of the singularity-free solutions for $\Lambda < 0$ in (g_r, g_s) plane. The top and bottom figures correspond to closed and open FLRW spacetime, respectively. The green and red regions indicate the solutions of $\mathcal{O}^{[-1;K]}$ and $\mathcal{O}^{[-1;-1]}_{\rm BC}$, respectively. $\mathcal{O}^{[-1;-1]}$ (ii) is located on the $\tilde{g}_s$ axis. The gray region is forbidden because the Hamiltonian constraint is never satisfied.

The typical forms of potentials and the distribution of the singularity-free solutions on $(\tilde{g}_r, \tilde{g}_s)$ plane are shown in Figs. 5 and 6, respectively.

IV. PERTURBATION ANALYSIS AROUND A NONFLAT FLRW BACKGROUND

In this section, we derive the perturbed quadratic action of the minimally extended nonprojectable HL theory. The perturbed ADM variables are defined by

$$N = \bar{N} + \delta N, \tag{4.1}$$

$$N_i = \bar{N}_i + \delta N_i, \tag{4.2}$$

$$g_{ij} = \bar{g}_{ij} + \delta g_{ij}, \tag{4.3}$$

with

$$\delta N = \alpha,$$
$$\delta N_i = \beta_i,$$
$$\delta g_{ij} = h_{ij} + \frac{1}{2}\bar{g}^{ab}h_{ai}h_{bj}, \tag{4.4}$$

where $\bar{N}$, $\bar{N}_i$ and $\bar{g}_{ij}$ denote the background lapse function, shift vector and three-dimensional induced metric, respectively. Furthermore, α, β_i and h_{ij} mean first-order perturbation of the above ADM variables. Note that indices of these perturbed variables are raised by $\bar{g}^{ij}$ as $h^i_j \coloneqq \bar{g}^{ia}h_{aj}$, $h^{ij} \coloneqq \bar{g}^{ia}\bar{g}^{jb}h_{ab}$, $h \coloneqq h^i_i = \bar{g}^{ia}h_{ia}$ and $\beta^i \coloneqq \bar{g}^{ia}\beta_a$.

A. Harmonic expansion

To decompose the perturbations into scalar, vector and tensor modes, we perform the harmonic expansion by equipping the set of tensor harmonics:

$$\mathbf{Y} = \{Q, Q_i, Q_{ij}, P_{ij}, S_{(o)i}, S_{(e)i}, S_{(o)ij}, S_{(e)ij}, G_{(o)ij}, G_{(e)ij}\}, \tag{4.5}$$

where Q, Q_i, Q_{ij}, P_{ij} are scalar-type harmonics. Q_{ij} and P_{ij} are trace and trace-less part, respectively. $S_{(o)i}$, $S_{(e)i}$, $S_{(o)ij}$, $S_{(e)ij}$ are vector-type harmonics. The symbols (o) and (e) correspond to the odd parity and the even parity, respectively. $G_{(o)ij}$, $G_{(e)ij}$ are tensor-type harmonics with the odd and the even parity. The explicit forms and these characteristics can be seen in Appendixes A and B in Ref. [48].

The scalar perturbations of the ADM variables are decomposed into

$$\alpha^{(\mathrm{scalar})} = \sum_{n,l,m}\alpha^{(n;lm)}_{(Q)}Q^{(n;lm)}, \tag{4.6}$$

$$\beta^{(\mathrm{scalar})}_i = \sum_{n,l,m}a^2[\beta^{(n;lm)}_{(Q)}Q^{(n;lm)}_i], \tag{4.7}$$

$$h^{(\mathrm{scalar})}_{ij} = \sum_{n,l,m}a^2[h^{(n;lm)}_{(Q)}Q^{(n;lm)}_{ij} + h^{(n;lm)}_{(P)}P^{(n;lm)}_{ij}], \tag{4.8}$$

the vector perturbations also can be expanded by

$$\beta^{(\mathrm{vector})}_i = \sum_{n,l,m}a^2[\beta^{(n;lm)}_{(S;o)}S^{(n;lm)}_{(o)i} + \beta^{(n;lm)}_{(S;e)}S^{(n;lm)}_{(e)i}], \tag{4.9}$$

$$h^{(\mathrm{vector})}_{ij} = \sum_{n,l,m}a^2[h^{(n;lm)}_{(S;o)}S^{(n;lm)}_{(o)ij} + h^{(n;lm)}_{(S;e)}S^{(n;lm)}_{(e)ij}], \tag{4.10}$$

and the tensor part is given by

$$h^{(\mathrm{tensor})}_{ij} = \sum_{n,l,m}a^2[h^{(n;lm)}_{(G;o)}G^{(n;lm)}_{(o)ij} + h^{(n;lm)}_{(G;e)}G^{(n;lm)}_{(e)ij}]. \tag{4.11}$$

where the degrees l, $m \in \mathbb{Z}$ are constrained by $0 \le l \le n-1$ and $0 \le |m| \le l$. $n \ge 1$ is a continuous real number for $K = 0, -1$, while a discrete natural number for $K = 1$.

Since we relax the projectability condition, the localness of the lapse perturbation α is recovered. Thus, we expand $\alpha^{(\mathrm{scalar})}$ by the harmonic functions.

B. Gauge fixing

Before calculating quadratic action, we have to remove the gauge degree of freedom (d.o.f.) from the perturbations. Since the HL theory respects the *foliation-preserving diffeomorphism* (2.1), the infinitesimal transformations of the perturbed ADM quantities are given by

$$\alpha^{(\mathrm{gauge})} = \partial_t f, \tag{4.12}$$

$$\beta^{(\mathrm{gauge})}_i = \partial_t\zeta_i - 2H\zeta_i, \tag{4.13}$$

$$h^{(\mathrm{gauge})}_{ij} = 2\nabla_{(i}\zeta_{j)} + 2Hf\bar{g}_{ij}. \tag{4.14}$$

We stress that f does not depend on space, thus, only ζ^i can be expanded by the harmonics:

$$\zeta_i = \sum_{n,l,m}a^2[\zeta^{(n;lm)}_{(Q)}Q^{(n;lm)}_i + \zeta^{(n;lm)}_{(S;o)}S^{(n;lm)}_{(o)i} + \zeta^{(n;lm)}_{(S;e)}S^{(n;lm)}_{(e)i}]. \tag{4.15}$$

Then, the infinitesimal gauge transformations of the harmonic expansion (4.6)–(4.11) are given by

$$pt\sum_{n,l,m}\alpha^{(n;lm)}_{(Q)}Q^{(n;lm)} \to \sum_{n,l,m}\alpha^{(n;lm)}_{(Q)}Q^{(n;lm)} + \partial_t f, \tag{4.16}$$

$$\beta^{(n;lm)}_{(Q)} \to \beta^{(n;lm)}_{(Q)} + \partial_t\zeta^{(n;lm)}_{(Q)}, \tag{4.17}$$

$$h^{(n;lm)}_{(P)} \to h^{(n;lm)}_{(P)} + \sqrt{\frac{8(\nu^2-3K)}{3}}\zeta^{(n;lm)}_{(Q)}, \tag{4.18}$$

$$\sum_{n,l,m}a^2h^{(n;lm)}_{(Q)}Q^{(n;lm)}_{ij} \to \sum_{n,l,m}a^2\left[h^{(n;lm)}_{(Q)} - \frac{2\nu}{\sqrt{3}}\zeta^{(n;lm)}_{(Q)}\right]Q^{(n;lm)}_{ij} + 2Hf\bar{g}_{ij}, \tag{4.19}$$

$$\beta^{(n;lm)}_{(S)} \to \beta^{(n;lm)}_{(S)} + \partial_t\zeta^{(n;lm)}_{(S)}, \tag{4.20}$$

$$h^{(n;lm)}_{(S)} \to h^{(n;lm)}_{(S)} + \sqrt{2(\nu^2-3K)}\zeta^{(n;lm)}_{(S)}, \tag{4.21}$$

$$h^{(n;lm)}_{(G)} \to h^{(n;lm)}_{(G)}. \tag{4.22}$$

where ν^2 is a eigenvalue of the harmonics which is defined by the following regions ($n \ge 1$):

$$\nu^2 \coloneqq \begin{cases} n^2-1, & n\in\mathbb{R} \quad \text{for } K=0 \\ n^2-1, & n\in\mathbb{N} \quad \text{for } K=1 \\ n^2+1, & n\in\mathbb{R} \quad \text{for } K=-1 \end{cases}. \tag{4.23}$$

Since both odd and even parity modes obey the same transformation law, the parity subscripts are abbreviated in vector and tensor perturbations.

We shall eliminate $h^{(n;lm)}_{(P)}$, $h^{(n;lm)}_{(S;o)}$ and $h^{(n;lm)}_{(S;e)}$ by choosing the following gauge

$$\zeta^{(n;lm)}_{(Q)} = -\left[\frac{8(\nu^2-3K)}{3}\right]^{-1/2} h^{(n;lm)}_{(P)}, \tag{4.24}$$

$$\zeta^{(n;lm)}_{(S;o)} = -[2(\nu^2-3K)]^{-1/2} h^{(n;lm)}_{(S;o)}, \tag{4.25}$$

$$\zeta^{(n;lm)}_{(S;e)} = -[2(\nu^2-3K)]^{-1/2} h^{(n;lm)}_{(S;e)}. \tag{4.26}$$

Unlike the projectable case, we cannot eliminate $\alpha^{(n;lm)}_{(Q)}$. In what follows, we have abbreviated the superscript $(n;lm)$ because the perturbed quantities do not mix with different modes.

C. Quadratic action

As is the case in the projectable HL theory, the quadratic action can be decomposed into the tensor part and the scalar one. The vector perturbations are not dynamical.

1. Tensor perturbations

Since the additional perturbation terms coming from $\mathcal{L}_{\rm NP}$ are only scalar modes, the tensor part of the quadratic action is identical to that of the projectable case:

$$\delta_{(2)}\mathcal{L}^{(\rm tensor)} = \frac{a^3}{2}[\mathcal{F}_{(G)}\dot{h}^2_{(G)} - \mathcal{G}_{(G)}h^2_{(G)}], \tag{4.27}$$

where we introduced $\mathcal{F}_{(G)}$ and $\mathcal{G}_{(G)}$ which can be regarded as the kinetic term and the mass term of the tensor perturbations, respectively. These variables, except for the total derivative terms, are given by

$$\mathcal{F}_{(G)} \coloneqq 1, \tag{4.28}$$

$$\mathcal{G}_{(G)} \coloneqq \frac{\nu^2}{a^2} + \frac{\nu^2}{3a^4}[-2g_rK + 3g_3\nu^2] + \frac{\nu^2}{a^6}[-g_sK^2 + 6g_{56}K\nu^2 + g_8\nu^2(\nu^2-2K)], \tag{4.29}$$

and we define $g_{56} \coloneqq g_5 + g_6$. The tensor quadratic action is defined for the case with $l \geq 2$, because the tensor harmonics $G^{(n;lm)}_{(o)ij}$ and $G^{(n;lm)}_{(e)ij}$ are vanished when $l < 2$.

2. Scalar perturbations

The scalar perturbations are drastically changed since the lapse perturbation $\alpha_{(Q)}$ cannot be eliminated by the gauge condition. Furthermore, $\mathcal{L}_{\rm NP}$ adds a new d.o.f. to scalar perturbations. The quadratic action of the scalar perturbations is given by

$$\begin{aligned}\delta_{(2)}\mathcal{L}^{(\rm scalar)} =& -\frac{a^3}{2}(3\lambda-1)\dot{h}^2_{(Q)} + \frac{a}{3}(\nu^2-3K)h^2_{(Q)} - \frac{1}{27a}(\nu^2-3K)[2g_r(2\nu^2-3K)+3g_3\nu^2]h^2_{(Q)} \\ & - \frac{1}{9a^3}(\nu^2-3K)[g_sK(4\nu^2-9K) + 2(3g_{56}-4g_7)K\nu^2 + (-8g_7+3g_8)\nu^2(3\nu^2-10K)]h^2_{(Q)} \\ & + 2\sqrt{3}a^3(3\lambda-1)H\dot{h}_{(Q)}\alpha_{(Q)} + \frac{4a}{\sqrt{3}}(\nu^2-3K)\left[1-\frac{2}{3a^2}g_rK - \frac{1}{a^4}K(g_sK-6g_7\nu^2)\right]h_{(Q)}\alpha_{(Q)} \\ & + 2a[\varsigma\nu^2 - 3a^2(3\lambda-1)H^2]\alpha^2_{(Q)} - (3\lambda-1)\frac{2\nu}{\sqrt{3}}\dot{h}_{(Q)}\beta_{(Q)} + 4a^3(3\lambda-1)\nu H\alpha_{(Q)}\beta_{(Q)} \\ & - 2a^3[(\lambda-1)\nu^2+2K]\beta^2_{(Q)}. \end{aligned} \tag{4.30}$$

We eliminated $\dot{H}$ by applying the scale factor equation (3.3). Since $\alpha_{(Q)}$ and $\beta_{(Q)}$ are not dynamical, we can eliminate both of them with the following constraint equations:

$$\beta_{(Q)} = \frac{(3\lambda-1)\nu}{(\lambda-1)\nu^2+2K}\left[H\alpha_{(Q)} - \frac{1}{2\sqrt{3}}\dot{h}_{(Q)}\right], \tag{4.31}$$

$$\alpha_{(Q)} = \frac{(\nu^2-3K)[((\lambda-1)\nu^2+2K)(3a^4-2g_rKa^2-3K(g_sK-6g_7\nu^2))h_{(Q)} - 3(3\lambda-1)Ha^6\dot{h}_{(Q)}]}{3\sqrt{3}a^4[\varsigma\nu^2((\lambda-1)\nu^2+2K) + 2(3\lambda-1)(\nu^2-3K)H^2a^2]}, \tag{4.32}$$

Substituting, (4.31) and (4.32) into (4.30), we achieve the quadratic action of scalar perturbations:

$$\delta_{(2)}\mathcal{L}^{(\mathrm{scalar})} = \frac{a^3}{2}[\mathcal{F}_{(Q)}\dot{h}^2_{(Q)} - \mathcal{G}_{(Q)}h^2_{(Q)}], \tag{4.33}$$

where

$$\mathcal{F}_{(Q)} := \frac{2\varsigma(3\lambda-1)\nu^2(\nu^2-3K)}{3\varsigma\nu^2[(\lambda-1)\nu^2+2K]+6(3\lambda-1)(\nu^2-3K)H^2a^2}, \tag{4.34}$$

$$\begin{aligned}\mathcal{G}_{(Q)} :=& -\frac{2}{3a^2}(\nu^2-3K)+\frac{2}{27a^4}(\nu^2-3K)[2g_r(2\nu^2-3K)+3g_3\nu^2]\\ &+\frac{2}{9a^6}(\nu^2-3K)[g_sK(4\nu^2-9K)+2(3g_{56}-4g_7)K\nu^2+(-8g_7+3g_8)\nu^2(3\nu^2-10K)]\\ &+\frac{4(\nu^2-3K)^2[(\lambda-1)\nu^2+2K](-3g_sK^2+18g_7K\nu^2-2g_rKa^2+3a^4)^2}{27a^{10}[\varsigma\nu^2\{(\lambda-1)\nu^2+2K\}+2(3\lambda-1)(\nu^2-3K)H^2a^2]}\\ &+\frac{8K(\nu^2-3K)^2(3g_sK^2+2g_rKa^2-3a^4)(3g_sK^2-18g_7K\nu^2+2g_rKa^2-3a^4)}{27a^{10}[\varsigma\nu^2\{(\lambda-1)\nu^2+2K\}+2(3\lambda-1)(\nu^2-3K)H^2a^2]}\\ &+\frac{4(3\lambda-1)(\nu^2-3K)^2H^2(3g_sK^2-18g_7K\nu^2-2g_rKa^2+9a^4)}{9a^4[\varsigma\nu^2\{(\lambda-1)\nu^2+2K\}+2(3\lambda-1)(\nu^2-3K)H^2a^2]}\\ &+\frac{32(3\lambda-1)(\nu^2-3K)^3H^2(-3g_sK^2+18g_7K\nu^2-2g_rKa^2+3a^4)(2g_sK^3+g_rK^2a^2-\Lambda a^6)}{27a^8[\varsigma\nu^2\{(\lambda-1)\nu^2+2K\}+2(3\lambda-1)(\nu^2-3K)H^2a^2]^2}.\end{aligned} \tag{4.35}$$

In closed FLRW spacetime, we focus only on the case with $n \geq 3$. Actually, the case with $n = 1$ corresponds to a constant shift of the scale factor, which is less important, and $n = 2$ is not dynamical mode. Thus, we can regard $(\nu^2 - 3K)$ as a positive value. It should be noted that, even if we take the limit $\varsigma \to 0$, we cannot replicate the quadratic scalar action in the projectable case (see (3.26) and (3.27) in Ref. [48]). In fact, a difference is caused by the gauge structure. As we have seen, $\alpha_{(Q)}$ is eliminated by applying constraint equation (4.31). Due to the recovering the local lapse function, it cannot be removed by global infinitesimal transformation f.

V. STABILITY ANALYSIS OF THE SINGULARITY-FREE SOLUTIONS

To examine whether a singularity-free cosmological solution is truly realized or not, it is essential to consider its stability. If the background solution is unstable with respect to small perturbations, the possibility of singularity avoidance may be spoiled. Thus, we examine the stabilities of singularity-free background solutions which are shown in previous section.

When we discuss the stability of a specific solution, the sign of $\mathcal{F}$ and $\mathcal{G}$ in the quadratic action provides guideposts (Since the discussion holds for both scalar and tensor modes, the subscripts are abbreviated.). The sign of $\mathcal{F}$ is relevant to the ghost instability. A perturbation mode with negative $\mathcal{F}$ losses the lowest energy state which leads the fatal collapse of the perturbative approach. Thus, we consider the condition $\mathcal{F} > 0$ as the absolute requirement.

On the other hand, the case with $\mathcal{G} < 0$ is, in general, regarded as the gradient instability. Such a situation corresponds to the negative squared mass, which seems to induce an exponential growth of perturbations. However, that unstable behavior may be suppressed by the effect of background dynamics. To clarify the effect from the background dynamics, we examine the perturbation equation of motions derived by taking variation of the quadratic action:

$$\ddot{h} + 3\mathcal{H}\dot{h} + \mathcal{M}^2 h = 0, \tag{5.1}$$

where

$$\mathcal{H} := H + \frac{\dot{\mathcal{F}}}{3\mathcal{F}}, \qquad \mathcal{M}^2 := \frac{\mathcal{G}}{\mathcal{F}}. \tag{5.2}$$

From the equation, one can see that the perturbation dynamics is influenced by the effective friction coefficient $\mathcal{H}$ as a background effect as well as the effective squared mass $\mathcal{M}^2$. The effective friction coefficients of the tensor perturbations $\mathcal{H}_{(G)}$ coincide with the Hubble parameter H, however, those of the scalar perturbations are not:

$$\mathcal{H}_{(Q)} = H\left(1 - \frac{4(\dot{H}+H^2)a^2}{3\varsigma\nu^2\left[\frac{(\lambda-1)\nu^2+2K}{(3\lambda-1)(\nu^2-3K)}\right]+6H^2a^2}\right). \tag{5.3}$$

We would like to stress that the positive $\mathcal{H}$ generates friction, on the other hand, the perturbations feel acceleration if $\mathcal{H}$

is negative. It is not completely determined by the Hubble parameter H unlike the projectable case. In what follows, the forces caused by $\mathcal{H} > 0$ and $\mathcal{H} < 0$ are called $\mathcal{H}$-friction and $\mathcal{H}$-acceleration, respectively.

Thus, we pay deep attention to the values of $\mathcal{M}^2$ and $\mathcal{H}$ to discuss the stability of the perturbations. In this paper, we classify the stabilities and instabilities into the following five types.

(i) Negative-$\mathcal{M}^2$ instability: As we mentioned, the negative $\mathcal{M}^2$ causes undesirable exponential growth unless it is not suppressed by the $\mathcal{H}$-friction. Therefore, the unstable behavior due to the negative $\mathcal{M}^2$ is observed in the case with (1) $\mathcal{M}^2 < 0$ and $\mathcal{H} < 0$, (2) $\mathcal{M}^2 < 0$ and $|\mathcal{M}^2| \gtrsim \mathcal{H}^2 > 0$ which means the effect of the third term in lhs of (5.1) is relatively dominant than that of the second term. If any one of the perturbation modes satisfies this condition, we classify the solution is under a negative-$\mathcal{M}^2$ instability.

(ii) $\mathcal{H}$-accelerated instability: Even if the squared effective mass is positive, it is possible to enhance the oscillating amplitude of perturbations. When $\mathcal{H} < 0$, the second term in lhs of (5.1) reinforces the amplitude rather than friction, thus the perturbation experiences a $\mathcal{H}$-acceleration. Clearly, the accelerating effect is manifested if the positive squared effective mass is relatively smaller than the effect of $\mathcal{H}$ term. Thus, we regard the solution is under a $\mathcal{H}$- accelerated instability if at least one of the perturbation modes satisfies $0 < \mathcal{M}^2 \lesssim \mathcal{H}^2$ and $\mathcal{H} < 0$.

(iii) $\mathcal{M}^2$- dominated stability: On the other hand, the negative $\mathcal{H}$ is not problematic if it is sufficiently suppressed by the heavy positive effective squared mass. Thus, we call the solution is under a $\mathcal{M}^2$-dominated stability if every perturbation mode satisfy $\mathcal{M}^2 \gtrsim \mathcal{H}^2$ and $\mathcal{H} < 0$.

(iv) $\mathcal{H}$-suppressed stability: If $\mathcal{H} > 0$, we experience a friction effect which suppresses the dynamics of the perturbations. With this taken into consideration, we can find a stable solution even if $\mathcal{M}^2 < 0$. That is, the effective squared mass is negative, however, the unstable behavior is suppressed by the positive $\mathcal{H}$. We call the solution is under a $\mathcal{H}$-suppressed stability if every perturbation mode satisfy $|\mathcal{M}^2| \lesssim \mathcal{H}^2$ and $\mathcal{M}^2 < 0$.

(v) Complete stability: Clearly, there is no problematic perturbation dynamics if every perturbation mode satisfy $\mathcal{M}^2 > 0$ and $\mathcal{H} > 0$. We call this situation complete stability.

In Table I, we summarize the classification of the stabilities and instabilities.

In principle, the types of stabilities are entirely determined by the coupling constants in the action. However, it is difficult to show the explicit conditions for these stabilities due to the complicated forms of $\mathcal{G}$ and $\mathcal{F}$ for general cases. Thus, we firstly consider the late-time evolutions after bounce in which $\mathcal{G}$ and $\mathcal{F}$ are quite simplified and the stability conditions are given in explicit forms. These explicit conditions can be imposed as necessary conditions for the stability throughout the whole evolution. Then, we numerically trace $\mathcal{G}$ and $\mathcal{F}$ based on the target background solutions.

TABLE I. The classification of stabilities and instabilities which is determined by $\mathcal{M}^2$ and $\mathcal{H}$.

Stability types	$\mathcal{H}$	$\mathcal{M}^2$	$\lvert\mathcal{M}^2\rvert \gtrsim \mathcal{H}^2$
Negative-$\mathcal{M}^2$ instability	$-$	$-$	False
	$-$	$-$	True
	$+$	$-$	True
$\mathcal{H}$-accelerated instability	$-$	$+$	False
$\mathcal{M}^2$-dominated stability	$-$	$+$	True
$\mathcal{H}$-suppressed stability	$+$	$-$	False
Complete stability	$+$	$+$	True
	$+$	$+$	False

A. Late-time universe after bounce

When the higher-order curvature terms are neglected, the forms of $\mathcal{G}$ and $\mathcal{F}$ are quite simplified. The tensor perturbations are approximated as

$$\mathcal{F}_{(G)} = 1, \qquad \mathcal{G}_{(G)} \approx \frac{\nu^2}{a^2} > 0, \tag{5.4}$$

which means these are under the complete stability. On the other hand, those of the scalar perturbations possibly take negative values. Therefore, we investigate the asymptotic forms of $\mathcal{G}$ and $\mathcal{F}$ in the late-time universe after bounce.

1. Asymptotic flat spacetime

Although it is impossible to realize a bounce solution in flat spacetime, it is expected to be an approximate solution inside the Hubble radius in the late-time of the Universe. Therefore, we examine the stability of the flat spacetime as an asymptotic spacetime after bounce. We assume $K = 0$, $\Lambda = 0$ and the scale factor is large, then, $\mathcal{F}_{(Q)}$ and $\mathcal{G}_{(Q)}$ are given by [53]

$$\mathcal{F}_{(Q)} = \frac{2\varsigma(3\lambda - 1)\nu^2}{3\varsigma(\lambda - 1)\nu^2 + 6(3\lambda - 1)H^2a^2}, \tag{5.5}$$

$$\mathcal{G}_{(Q)} \approx \frac{2(2 - \varsigma)\nu^2}{3\varsigma a^2}. \tag{5.6}$$

Since $\mathcal{G}_{(Q)}$ cannot be positive if $\varsigma < 0$, we focus only on the case with $\varsigma > 0$. To preserve $\mathcal{F}_{(Q)} > 0$ and $\mathcal{G}_{(Q)} > 0$, we must impose

$$\lambda > 1 \quad \text{and} \quad 0 < \varsigma < 2. \tag{5.7}$$

Then, the solutions are under the complete stability.

2. Asymptotic Milne spacetime

The Milne universe is also a solution of open FLRW spacetime without a cosmological constant in deep infrared regime. The scale factor evolves as

$$a \sim \sqrt{\frac{2}{3\lambda-1}}t. \tag{5.8}$$

Then, $\mathcal{F}_{(Q)}$ and $\mathcal{G}_{(Q)}$ are approximated by

$$\mathcal{F}_{(Q)} \approx \frac{2\varsigma(3\lambda-1)\nu^2(\nu^2+3)}{3[\varsigma(\lambda-1)\nu^4+2(2-\varsigma)\nu^2+12]}, \tag{5.9}$$

$$\mathcal{G}_{(Q)} \approx \frac{2\nu^2(\nu^2+3)}{3a^2} \times \left[\frac{(2-\varsigma)(\lambda-1)\nu^2+2\varsigma+6(\lambda-1)}{\varsigma(\lambda-1)\nu^4+2(2-\varsigma)\nu^2+12}\right]. \tag{5.10}$$

Then, the conditions for the positive $\mathcal{F}_{(Q)}$ and $\mathcal{G}_{(Q)}$ are given by

$$\lambda \geq 1 \quad \text{and} \quad 0 < \varsigma < 2. \tag{5.11}$$

The important point is we can stabilize asymptotic spacetime after bounce without cosmological constant unlike the projectable case.

We also analyze the asymptotic dynamics of the perturbations. The asymptotic behaviors of the effective friction coefficients are given by

$$\mathcal{H}^2_{(G)} \sim \frac{1}{t^2}, \tag{5.12}$$

$$\mathcal{H}^2_{(Q)} \sim \frac{1}{t^2}, \tag{5.13}$$

and those of the effective squared masses are reduced into

$$\mathcal{M}^2_{(G)}a^2 \sim \frac{(3\lambda-1)\nu^2}{2}, \tag{5.14}$$

$$\mathcal{M}^2_{(Q)}a^2 \sim \frac{(2-\varsigma)(\lambda-1)\nu^2+2\varsigma+6(\lambda-1)}{2\varsigma}. \tag{5.15}$$

Then, the asymptotic dynamics of the perturbations are approximated by the following form:

$$h \sim \frac{C_1}{t}\cos\left[\sqrt{\mathcal{M}^2a^2-1}\,\ln t\right]+\frac{C_2}{t}\sin\left[\sqrt{\mathcal{M}^2a^2-1}\,\ln t\right], \tag{5.16}$$

with integration constants C_1 and C_2. One can see that the perturbation amplitude approaches to zero.

3. Asymptotic de Sitter spacetime

If a positive cosmological constant is present, it may be possible that the Universe experiences an accelerating expansion whose expanding law is given by

$$a \sim \exp\left(\sqrt{\frac{2\Lambda}{3(3\lambda-1)}}t\right). \tag{5.17}$$

Once the Universe enters the accelerating expansion phase, the spatial curvature turns to be irrelevant within a few Hubble time, then, the spacetime asymptotically approaches to de Sitter spacetime. In that case, $\mathcal{F}_{(Q)}$ and $\mathcal{G}_{(Q)}$ are approximated by[3]

$$\mathcal{F}_{(Q)} \approx \frac{\varsigma\nu^2}{3H^2a^2}, \tag{5.18}$$

$$\mathcal{G}_{(Q)} \approx \frac{2\nu^2}{27a^4}\left[\frac{27(2+\varsigma)}{4\Lambda}((\lambda-1)\nu^2+2K) + (\nu^2-3K)(4g_r+3g_3)\right]. \tag{5.19}$$

The positivity of $\mathcal{F}_{(Q)}$ is satisfied if $\varsigma > 0$ which is consistent with that of in the asymptotic flat spacetime. We show the explicit conditions for $\mathcal{G}_{(Q)} \geq 0$ in closed spacetime:

$$3g_3+4g_r+\frac{27(\lambda-1)(2+\varsigma)}{4\Lambda} \geq 0. \tag{5.20}$$

and in open spacetime:

$$3g_3+4g_r+\frac{27(\lambda-2)(2+\varsigma)}{10\Lambda} \geq 0. \tag{5.21}$$

If the above condition is satisfied, the solutions are under the complete stability in the asymptotic de Sitter era.

It is clear that the squared effective masses $\mathcal{M}^2_{(Q)}$ approach asymptotically to zero because it is proportional to a^{-2}. Therefore, the case with $\mathcal{G}_{(Q)} < 0$ seems not to be quite problematic because the solution is under the $\mathcal{H}$-suppressed stability. To confirm it, we examine the asymptotic dynamics of the perturbations. The effective friction coefficients asymptotically behave as

$$\mathcal{H}^2_{(G)} \sim \frac{2\Lambda}{3(3\lambda-1)}, \tag{5.22}$$

[3]It is natural to consider that there exists an ultraviolet cutoff momentum $p_{\rm cut}$ at which a nonperturbative quantum effect of gravity cannot be ignored. More precisely, let $\nu_{\rm cut}$ be an ultraviolet cutoff mode which is related with the cutoff momentum as $\nu^2_{\rm cut}/a^2_T \approx p^2_{\rm cut}$ at the early stage of the Universe. Then, we find some finite time so that $\nu^2/a^2 < H^2$ for any $\nu \leq \nu_{\rm cut}$. Therefore, the all perturbation modes are rapidly suppressed by the strong $\mathcal{H}$-friction after that time.

$$\mathcal{H}^2_{(Q)} \sim \frac{2\Lambda}{27(3\lambda-1)}, \tag{5.23}$$

and those of the effective squared masses are

$$\mathcal{M}^2_{(G)}a^2 \sim \nu^2, \tag{5.24}$$

$$\mathcal{M}^2_{(Q)}a^2 \sim \frac{2H^2}{9\varsigma}\left[\frac{27(2+\varsigma)}{4\Lambda}((\lambda-1)\nu^2+2K) + (\nu^2-3K)(4g_r+3g_3)\right]. \tag{5.25}$$

Substituting them into the perturbation equations of motion, we obtain the asymptotic behaviors. For the case with $\mathcal{M}^2 > 0$, which means the perturbations are under the complete stability, the asymptotic dynamics of the tensor perturbations are

$$h_{(G)} \sim \left[C_3\sqrt{\frac{\mathcal{M}^2_{(G)}a^2}{H^2}}e^{-Ht}+C_4\right]\cos\left(\sqrt{\frac{\mathcal{M}^2_{(G)}a^2}{H^2}}e^{-Ht}\right) - \left[C_3-C_4\sqrt{\frac{\mathcal{M}^2_{(G)}a^2}{H^2}}e^{-Ht}\right]\sin\left(\sqrt{\frac{\mathcal{M}^2_{(G)}a^2}{H^2}}e^{-Ht}\right), \tag{5.26}$$

and those of the scalar perturbations are given by

$$h_{(Q)} \sim C_5\cos\left(\sqrt{\frac{\mathcal{M}^2_{(Q)}a^2}{H^2}}e^{-Ht}\right) - C_6\sin\left(\sqrt{\frac{\mathcal{M}^2_{(Q)}a^2}{H^2}}e^{-Ht}\right), \tag{5.27}$$

with integration constants C_3, C_4, C_5 and C_6. We find that the perturbations are rapidly suppressed and settled into some constants as $h_{(G)} \sim C_4$ and $h_{(Q)} \sim C_5$. Since the constants C_4 and C_5 are expected to be a typical amplitude of the perturbations when the Universe enters the de Sitter era, we generally observe nonzero value of perturbation amplitude after entering de Sitter phase.

For the case with $\mathcal{M}^2 < 0$, the dynamics of the tensor perturbations are approximated as

$$h_{(G)} \sim \left[C_7\sqrt{\frac{|\mathcal{M}^2_{(G)}a^2|}{H^2}}e^{-Ht}+C_8\right]\times\cosh\left(\sqrt{\frac{|\mathcal{M}^2_{(G)}a^2|}{H^2}}e^{-Ht}\right) - \left[C_7-C_8\sqrt{\frac{|\mathcal{M}^2_{(G)}a^2|}{H^2}}e^{-Ht}\right]\times\sinh\left(\sqrt{\frac{|\mathcal{M}^2_{(G)}a^2|}{H^2}}e^{-Ht}\right), \tag{5.28}$$

and those of the scalar perturbations are given by

$$h_{(Q)} \sim C_9\cosh\left(\sqrt{\frac{|\mathcal{M}^2_{(Q)}a^2|}{H^2}}e^{-Ht}\right) - C_{10}\sinh\left(\sqrt{\frac{|\mathcal{M}^2_{(Q)}a^2|}{H^2}}e^{-Ht}\right), \tag{5.29}$$

with integration constants C_7, C_8, C_9 and C_{10}. Then, we also find that the perturbations are rapidly settled into some constant as $h_{(G)} \sim C_8$ and $h_{(Q)} \sim C_9$, which means the $\mathcal{H}$-suppressed stability is truly stabilized state.

B. Whole history of the Universe

Let us turn our attention to the whole history of the Universe including the bouncing phase. Although our main analysis depends on the numerical approach, we, in advance, consider some simple specific cases again in which explicit conditions can be derived.

1. Tensor perturbations

Since the coefficients of kinetic terms in tensor perturbations are unity, these are free from the ghost instability. Therefore, the stabilities are determined only by $\mathcal{G}_{(G)}$. As we mentioned, the forms of $\mathcal{F}_{(G)}$ and $\mathcal{G}_{(G)}$ in tensor perturbation are identical to those of the projectable case. Thus, we summarize the positivity conditions of $\mathcal{G}_{(G)}$, which we have argued in previous paper [48].

To investigate the stability of the tensor perturbations, we focus on the case with large ν^2. Then, $\mathcal{G}_{(G)}$ given in (4.29) is approximated as

$$\mathcal{G}_{(G)} \sim \frac{\nu^2}{a^2} + g_3\frac{\nu^4}{a^4} + g_8\frac{\nu^6}{a^6}. \tag{5.30}$$

One can see that the ultraviolet stability imposes $g_8 \geq 0$.

Although the explicit condition for general case is quite complicated, we show the conditions with $g_3 = 0$. In closed spacetime ($K = 1$), if one of the following conditions is satisfied, $\mathcal{G}_{(G)}$ must be positive for any $a > 0$ and $\nu^2 \geq 8$:

$$\text{(i)}\quad 0 < g_8 \leq -\frac{3g_{56}}{7},\quad g_r < 0,\quad g_s \leq -\frac{(g_8 - 3g_{56})^2}{g_8};$$

$$\text{(ii)}\quad 0 < g_8 \leq -\frac{3g_{56}}{7},\quad g_r \geq 0,\quad g_s \leq -\frac{(g_8 - 3g_{56})^2}{g_8} - \frac{g_r^2}{9};$$

$$\text{(iii)}\quad 0 \leq g_8,\quad -\frac{3g_{56}}{7} < g_8,\quad g_r < 0,\quad g_s \leq 48(g_{56} + g_8);$$

$$\text{(iv)}\quad 0 \leq g_8,\quad -\frac{3g_{56}}{7} < g_8,\quad g_r \geq 0,\quad g_s \leq 48(g_{56} + g_8) - \frac{g_r^2}{9};$$

Similarly, in open spacetime ($K = -1$):

$$\text{(i)}\quad 0 < g_8 \leq g_{56},\quad g_r > 0,\quad g_s \leq -\frac{(g_8 - 3g_{56})^2}{g_8};$$

$$\text{(ii)}\quad 0 < g_8 \leq g_{56},\quad g_r \leq 0,\quad g_s \leq -\frac{(g_8 - 3g_{56})^2}{g_8} - \frac{g_r^2}{9};$$

$$\text{(iii)}\quad 0 \leq g_8,\quad g_{56} < g_8,\quad g_r > 0,\quad g_s \leq 4(2g_8 - 3g_{56});$$

$$\text{(iv)}\quad 0 \leq g_8,\quad g_{56} < g_8,\quad g_r \leq 0,\quad g_s \leq 4(2g_8 - 3g_{56}) - \frac{g_r^2}{9},$$

which are equivalent to $\mathcal{G}_{(G)} \geq 0$ for any $a > 0$ and $\nu^2 \geq 2$. It is worth mentioning that these stability conditions in open FLRW spacetime are not completely conflict, however slightly difficult to be compatible with the bouncing conditions (see [48]).

2. Scalar perturbations

The ghost-free condition for scalar perturbations can be analytically discussed [refer to (4.34)]. Let the coupling constants be $\lambda > 1/3$ and $\varsigma > 0$, and adopting $\nu^2 - 3K > 0$, the condition $\mathcal{F}_{(Q)} > 0$ is equivalent to

$$\frac{\varsigma\nu^2[(\lambda - 1)\nu^2 + 2K]}{2(3\lambda - 1)(\nu^2 - 3K)a^2} > -H^2. \tag{5.31}$$

The most stringent conditions are imposed at the bouncing and the recollapse points, i.e., $H = 0$:

$$\varsigma > 0 \quad \text{and} \quad \begin{cases} \lambda > 1 & \text{for } K = 0 \\ \lambda \geq 1 & \text{for } K = 1 \\ \lambda > 2 & \text{for } K = -1 \end{cases}. \tag{5.32}$$

If the above conditions are satisfied, the ghost instability can be eliminated throughout the evolution of the Universe.

On the other hand, the positivity conditions of $\mathcal{G}_{(Q)}$ cannot be expressed without any approximation due to the extremely complicated form as shown in (4.35). Therefore, we restrict our analysis to the case with large ν^2 modes at this stage. Then, $\mathcal{G}_{(Q)}$ is given by

$$\mathcal{G}_{(Q)} \approx \left[(-8g_7 + 3g_8) + \frac{72g_7^2K^2}{\varsigma a^4}\right]\frac{2\nu^6}{3a^6}, \tag{5.33}$$

Since ς should be positive, we assume

$$3g_8 \geq 8g_7. \tag{5.34}$$

Then, $\mathcal{G}_{(Q)} \geq 0$ for large ν is guaranteed.

3. Numerical analysis

Before performing the numerical analysis, we summarize the necessary conditions of stable solutions for each case.

(1) The cases with $K = 1$ and $\Lambda \leq 0$: Since there exists a finite maximum value of scale factor $a_{\max}$, i.e., the solutions $\mathcal{O}^{[0;1]}$ and $\mathcal{O}^{[-1;1]}$, we assume the stability conditions around the bouncing and the recollapsing points and in the large ν^2 region, thus,

$$\varsigma > 0,\quad \lambda \geq 1,\quad g_8 \geq 0 \quad \text{and} \quad 3g_8 \geq 8g_7. \tag{5.35}$$

(2) The cases with $K = 1$ and $\Lambda > 0$: In this cases, we observe $\mathcal{B}^{[1;1]}$, $\mathcal{B}_{\mathrm{BC}}^{[1;1]}$ and $\mathcal{B}_{\mathrm{O}}^{[1;1]}$ as the singularity-free solutions. To guarantee the stabilities around bouncing point (and the recollapsing point if $\mathcal{B}_{\mathrm{O}}^{[1;1]}$), in asymptotic de Sitter spacetime and in the large ν^2 region, we assume

$$\varsigma > 0,\quad \lambda \geq 1,\quad 3g_3 + 4g_r + \frac{27(\lambda - 1)(2 + \varsigma)}{4\Lambda} \geq 0,$$
$$g_8 \geq 0 \quad \text{and} \quad 3g_8 \geq 8g_7. \tag{5.36}$$

If we focus only on the oscillating phase which is observed in the solution $\mathcal{B}_{\mathrm{O}}^{[1;1]}$, the stability conditions in the asymptotic de Sitter spacetime can be relaxed. Then, we impose the same conditions as the cases with $K = 1$ and $\Lambda \leq 0$, that is, (5.35).

(3) The cases with $K = -1$ and $\Lambda = 0$: We find $\mathcal{B}^{[0,-1]}$ and $\mathcal{B}_{\mathrm{BC}}^{[0,-1]}$ as the singularity-free solutions whose asymptotic behaviors are the Milne spacetime. Thus, we impose

$$0 < \varsigma < 2,\quad \lambda > 2,\quad g_8 \geq 0 \quad \text{and} \quad 3g_8 \geq 7g_7. \tag{5.37}$$

(4) The cases with $K = -1$ and $\Lambda > 0$: In this case, the solutions $\mathcal{B}^{[1,-1]}$ and $\mathcal{B}_{\mathrm{BC}}^{[1,-1]}$ are realized. Since both of the solutions approaches the de Sitter spacetime after

TABLE II. The examples for the stable singularity-free solutions, which mean that these solutions are under the $\mathcal{M}^2$-dominated stability when $\mathcal{H}<0$ and under the complete stability when $\mathcal{H}>0$. The types of solution are introduced in Sec. III. N/A means that there is no corresponding variables.

	Type	Λ	λ	g_2	g_3	g_4	g_5	g_6	g_7	g_8	ς	g_r	g_s	$a_{\rm BC}$	$a_{\rm min}$	$a_{\rm max}$	a_T
(i)	$\mathcal{O}^{[0;1]}$	0	1	$-\frac{1}{18}$	$\frac{1}{3}$	$-\frac{1}{108}$	0	$\frac{7}{90}$	$\frac{1}{2}$	1	1	1	$-\frac{1}{15}$	N/A	0.304	0.491	N/A
(ii)	$\mathcal{B}^{[0;-1]}$	0	6	$-\frac{1}{18}$	$\frac{1}{8}$	0	$\frac{1}{3}$	$-\frac{2}{3}$	-1	3	$\frac{3}{2}$	$-\frac{1}{4}$	4	N/A	N/A	N/A	1.094
(iii)	$\mathcal{B}^{[0;-1]}_{\rm BC}$	0	$\frac{5}{2}$	$-\frac{1}{18}$	$-\frac{1}{3}$	$\frac{1}{20}$	$-\frac{1}{4}$	$\frac{1}{4}$	0	1	$\frac{1}{2}$	-3	$-\frac{3}{5}$	0.526	N/A	N/A	0.851
(iv)	$\mathcal{B}^{[1;1]}$	1	1	$\frac{1}{6}$	$-\frac{1}{6}$	$-\frac{1}{12}$	$\frac{1}{3}$	$-\frac{1}{3}$	$-\frac{1}{2}$	1	$\frac{3}{2}$	2	-1	N/A	N/A	N/A	1.525
(v)	$\mathcal{B}^{[1;1]}_{\rm BC}$	2	2	$\frac{1}{9}$	$-\frac{1}{2}$	$-\frac{1}{12}$	$\frac{1}{3}$	$-\frac{1}{6}$	$-\frac{1}{2}$	1	1	-1	1	0.707	N/A	N/A	1.272
(vi)	$\mathcal{B}^{[1;1]}_{\rm O}$	2	1	$\frac{2}{45}$	0	$-\frac{1}{108}$	$\frac{2}{75}$	0	0	2	$\frac{1}{2}$	$\frac{4}{5}$	$-\frac{1}{25}$	N/A	0.256	0.511	1.083
(vii)	$\mathcal{B}^{[1;-1]}$	1	$\frac{5}{2}$	0	$-\frac{1}{6}$	0	$\frac{1}{6}$	$-\frac{1}{3}$	$\frac{1}{2}$	2	1	-1	2	N/A	N/A	N/A	0.928
(viii)	$\mathcal{B}^{[1;-1]}_{\rm BC}$	2	3	$-\frac{1}{3}$	$\frac{1}{2}$	$-\frac{1}{30}$	$\frac{1}{5}$	$-\frac{1}{3}$	-1	1	$\frac{3}{2}$	-3	$-\frac{2}{5}$	0.403	N/A	N/A	0.745
(ix)	$\mathcal{O}^{[-1;1]}$	-1	1	$-\frac{1}{12}$	$\frac{1}{2}$	$-\frac{1}{108}$	$\frac{1}{40}$	0	1	1	1	$\frac{3}{2}$	$-\frac{1}{10}$	N/A	0.282	0.604	N/A
(x)	$\mathcal{O}^{[-1;-1]}$	-1	3	$\frac{1}{4}$	$-\frac{1}{2}$	0	$-\frac{1}{40}$	$\frac{1}{5}$	0	3	1	$\frac{3}{2}$	$\frac{3}{2}$	N/A	0.730	1.821	N/A
(xi)	$\mathcal{O}^{[-1;-1]}_{\rm BC}$	$-\frac{3}{2}$	$\frac{5}{2}$	$\frac{1}{8}$	$-\frac{1}{2}$	$\frac{1}{216}$	$-\frac{1}{60}$	$\frac{1}{150}$	-1	2	$\frac{1}{2}$	$-\frac{3}{4}$	$-\frac{1}{50}$	0.174	0.507	1.309	N/A

the bounce, we impose the conditions as follows:

$$\varsigma>0,\quad \lambda>2,\quad 3g_3+4g_r+\frac{27(\lambda-2)(2+\varsigma)}{10\Lambda}\geq 0,$$
$$g_8\geq 0\quad\text{and}\quad 3g_8\geq 8g_7. \tag{5.38}$$

(5) The cases with $K=-1$ and $\Lambda<0$: The possible singularity-free solutions are $\mathcal{O}^{[-1;-1]}$ and $\mathcal{O}^{[-1;-1]}_{\rm BC}$. Therefore, we impose the stability conditions around the bouncing and recollapsing points and in the large ν^2 region:

$$\varsigma>0,\quad \lambda>2,\quad g_8\geq 0\quad\text{and}\quad 3g_8\geq 8g_7. \tag{5.39}$$

Then, we shall investigate the spacetime stabilities in each cases: bouncing solutions with asymptotic de Sitter spacetime, bouncing solutions with asymptotic Milne spacetime and oscillating solutions. In our numerical analysis, we have found stable singularity-free solutions throughout the whole evolutions, which means these solutions are under the $\mathcal{M}^2$-dominated stability when $\mathcal{H}<0$ and under the complete stability when $\mathcal{H}>0$. The important point is that such stable solutions seem to exist universally. In fact, all types of background solutions which we have introduced in Sec. III B can be stabilized. The concrete examples are shown in Table II.

Bouncing solutions with asymptotic Milne spacetime.— The solutions $\mathcal{B}^{[0;-1]}$ and $\mathcal{B}^{[0;-1]}_{\rm BC}$ correspond to this case. Recall that these types of singularity-free solutions cannot be stabilized in the projectable HL theory. Since the Hubble parameter is dropped as $t^{-1}\sim a^{-1}$, the effect of the squared effective masses do not suppressed by the Hubble friction, that is, the values of $\mathcal{M}^2/H^2$ are negative constants and do not approach to zero at asymptotic Milne regime.

On the other hand, we can discover the stable solutions in the nonprojectable HL theory because it is possible to keep the values of $\mathcal{M}^2_{(Q)}$ to be positive during the whole evolution. In Fig. 7, a typical example of such a solution is shown. The figure shows that $\mathcal{M}^2/\mathcal{H}^2$ of both tensor and scalar perturbations keep the positive values and always greater than unity. Thus, the $\mathcal{H}$-accelerated instability does not occur for any initial value of the scale factor $a_{\rm ini}$. As far as our numerical analysis is concerned, such behavior can also be seen for any possible perturbation mode ν. Therefore, we regard our example as a solution under complete stability when $\mathcal{H}>0$ and under $\mathcal{M}^2$-dominated stability when $\mathcal{H}<0$ for any $a_{\rm ini}$.

One may wonder whether the squared effective masses truly suppress the effects of $\mathcal{H}$-acceleration under the $\mathcal{M}^2$-dominated stability, because we do not mention any explicit criterions of the ratio $\mathcal{M}^2/\mathcal{H}^2$ so far. Thus, we additionally discuss the dynamical evolutions of each perturbation modes to investigate the growth of the perturbation amplitudes caused by the $\mathcal{H}$-acceleration.

To clarify the effects, we numerically solve the perturbation equations of motion (5.1). The initial conditions are given at $a_{\rm ini}=100a_T$ so that $\dot{h}_{(G)}=0=\dot{h}_{(Q)}$. Since the equations of motion are linear with respect to $h_{(G)}$ and $h_{(Q)}$, the whole evolutions are proportional to the values of the initial conditions $h_{(G)\rm ini}$ and $h_{(Q)\rm ini}$. Therefore, we trace the ratios to each initial values, i.e., $h_{(G)}/h_{(G)\rm ini}$ and $h_{(Q)}/h_{(Q)\rm ini}$. In Fig. 8, the time evolutions are shown. This result is based on the solution $\mathcal{B}^{[0;-1]}$ whose coupling constants are given in Table II (ii), thus, also corresponds with Fig. 7. From the figure, we find that the perturbation amplitudes are enhanced around the bouncing point even if

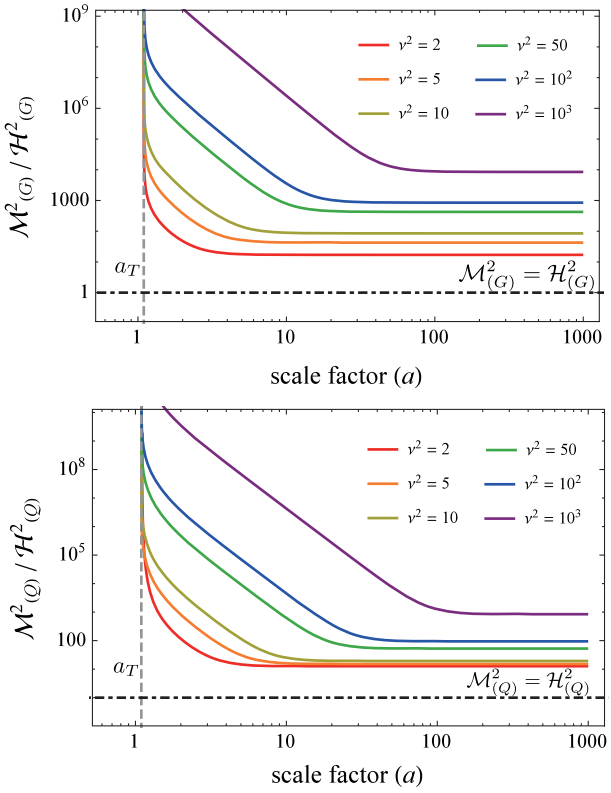

FIG. 7. The typical example of the ratios of the squared effective mass to the squared effective friction coefficient $\mathcal{M}^2/\mathcal{H}^2$ in the bouncing solution with asymptotic Milne spacetime. The top and the bottom figures stands for $\mathcal{M}^2_{(G)}/\mathcal{H}^2_{(G)}$ and $\mathcal{M}^2_{(Q)}/\mathcal{H}^2_{(Q)}$, respectively. The example solution is $\mathcal{B}^{[0;-1]}$ whose values of coupling constants are given in Table II (ii). The red, orange, yellow, green, blue and purple curves indicate the evolutions with $\nu^2 = 2$, 5, 10, 50, 10^2 and 10^3, respectively ($\nu^2 = n^2 + 1$). The horizontal dot-dashed black lines indicate $\mathcal{M}^2 = \mathcal{H}^2$. The vertical dashed gray line indicates the bouncing radius.

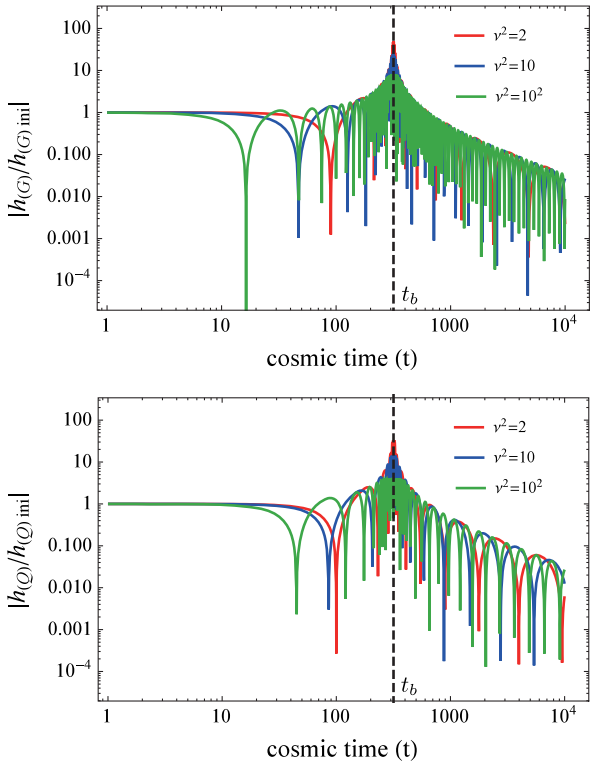

FIG. 8. The evolutions of perturbations in the bouncing solution $\mathcal{B}^{[0;-1]}$ where the coupling constants are listed in Table II (ii). In the top (bottom) figure, the evolution of tensor (scalar) perturbations are illustrated. The initial conditions are selected by $a_{\mathrm{ini}} = 100a_T \approx 109.41$, and $\dot{h}_{(G)} = 0 = \dot{h}_{(Q)}$. The red, blue and green curves correspond to $\nu^2 = 2$, 10 and 100, respectively. The vertical dashed black line means the time of bouncing $t_b \approx 317.19$.

the solution is under the $\mathcal{M}^2$-dominated stability. Thus, we should clarify the growth rates of the perturbations. In Table III, we show the detail data of the maximum ratios $h_{(G)}/h_{(G)\mathrm{ini}}$ and $h_{(Q)}/h_{(Q)\mathrm{ini}}$ throughout the evolutions for each perturbation modes. From the data, the amplitude possibly grows up to about 50 times and tends to be higher as the perturbation mode ν^2 is lower. Since the large perturbation mode ν^2 corresponds to the heavy effective squared mass $\mathcal{M}^2$, the result seems appropriate.

TABLE III. The maximum ratios $h_{(G)}/h_{(G)\mathrm{ini}}$ and $h_{(Q)}/h_{(Q)\mathrm{ini}}$ throughout the evolutions for each perturbation modes based on Table II (ii).

ν^2	$\max(h_{(G)}/h_{(G)\mathrm{ini}})$	$\max(h_{(Q)}/h_{(Q)\mathrm{ini}})$
2	49.425	32.907
5	33.761	20.835
10	24.876	13.945
50	11.612	5.933
100	8.263	4.132
300	4.795	2.308

Bouncing solutions with asymptotic de Sitter spacetime.— The solutions $\mathcal{B}^{[1;1]}$, $\mathcal{B}^{[1;1]}_{\mathrm{BC}}$, $\mathcal{B}^{[1;1]}_{\mathrm{O}}$ with $a \geq a_T$, $\mathcal{B}^{[1;-1]}$ and $\mathcal{B}^{[1;-1]}_{\mathrm{BC}}$ correspond to this case. Actually, the previous work based on the projectable HL theory has shown that we cannot construct a solution under the complete stability. Instead of this, it is possible to find solutions under the $\mathcal{H}$-suppressed stability due to the negative $\mathcal{M}^2_{(Q)}$ in infrared regime.

On the other hand, it turns out that solutions under the complete stability can be realized in the nonprojectable case. As an example, we show the evolutions of the $\mathcal{M}^2/\mathcal{H}^2$ in Fig. 9. As can be seen from the figure, both tensor and scalar perturbations keep the positive values during whole evolution of the solution. As far as our analysis is concerned, the squared effective masses of tensor and scalar perturbations are monotonically

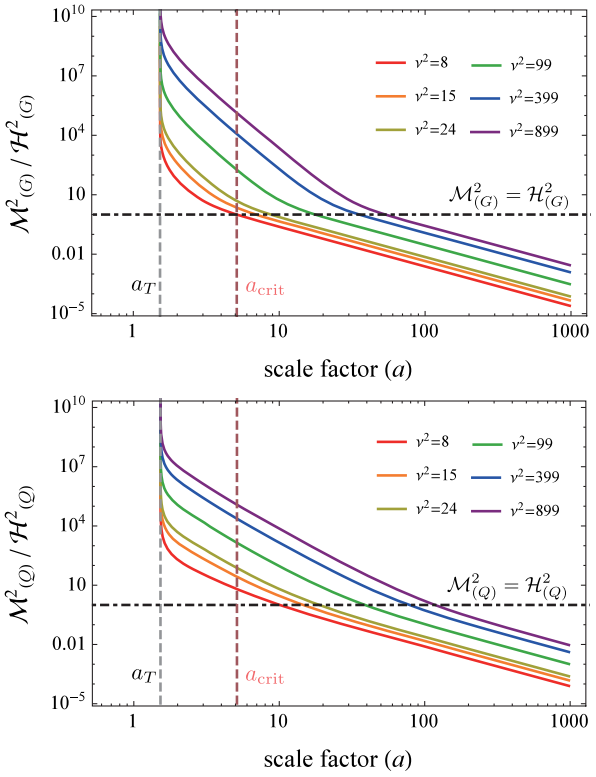

FIG. 9. The typical example of the ratios of the squared effective mass to the squared effective friction coefficient $\mathcal{M}^2/\mathcal{H}^2$ in the bouncing solution with asymptotic de Sitter spacetime. The top and the bottom figures stands for $\mathcal{M}^2_{(G)}/\mathcal{H}^2_{(G)}$ and $\mathcal{M}^2_{(Q)}/\mathcal{H}^2_{(Q)}$, respectively. The example solution is $\mathcal{B}^{[1;1]}$ whose values of coupling constants are given in Table II (iv). The red, orange, yellow, green, blue and purple curves indicate the evolutions with $\nu^2 = 8$, 15, 24, 99, 399 and 899, respectively ($\nu^2 = n^2 - 1$). The horizontal dot-dashed black lines indicate $\mathcal{M}^2 = \mathcal{H}^2$. The vertical dashed gray line gives the bouncing radius, while the vertical dashed pink line shows the critical scale factor $a_{\rm crit} = 5.118$.

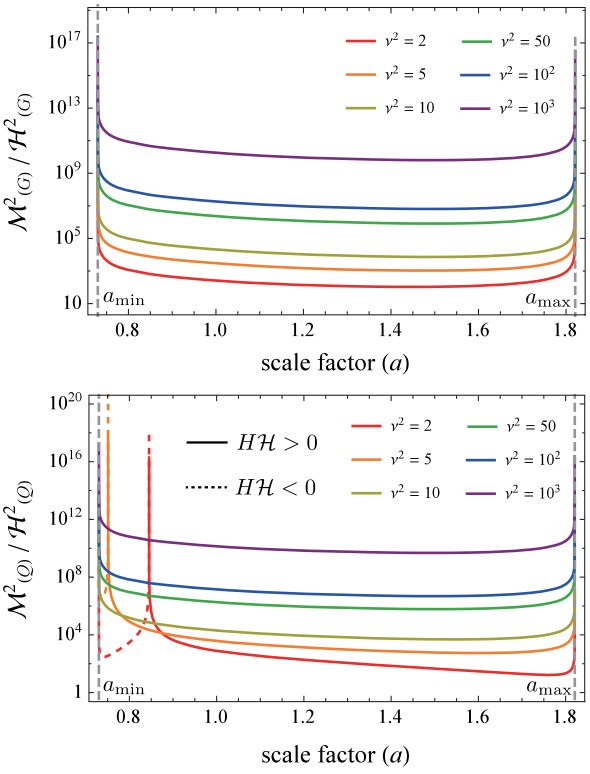

FIG. 10. The typical example of the ratios of the squared effective mass to the squared effective friction coefficient $\mathcal{M}^2/\mathcal{H}^2$ in the oscillating solution. The top and the bottom figures stands for $\mathcal{M}^2_{(G)}/\mathcal{H}^2_{(G)}$ and $\mathcal{M}^2_{(Q)}/\mathcal{H}^2_{(Q)}$, respectively. The example solution is $\mathcal{O}^{[-1;-1]}$ whose values of coupling constants are given in Table II (x). The red, orange, yellow, green, blue and purple curves indicate the evolutions with $\nu^2 = 2$, 5, 10, 50, 10^2 and 10^3, respectively ($\nu^2 = n^2 + 1$). The solid and dashed colored curves represent the evolutions with $H\mathcal{H} > 0$ and $H\mathcal{H} < 0$, respectively. The vertical dashed gray lines indicate the maximum and minimum radii of the oscillation.

increasing functions with respect to the perturbation mode ν^2. Therefore, we conclude this solution is under complete stability for any possible ν^2.

The magnitude relationships between $\mathcal{M}^2$ and $\mathcal{H}^2$ are also analyzed. As we discussed, both $\mathcal{M}^2_{(G)}$ and $\mathcal{M}^2_{(Q)}$ drop as a^{-2}, in contrast, the effective friction coefficients are settled to a constant. Thus, there must exist a certain value of the scale factor such that any one of $\mathcal{M}^2$ is equal to $\mathcal{H}^2$. We define such a value of scale factor as a critical scale factor $a_{\rm crit}$. In our numerical example Fig. 9, the critical scale factor is $a_{\rm crit} = 5.118$ at which the lowest ν^2 mode of the tensor perturbation shows $\mathcal{M}^2_{(G)} = \mathcal{H}^2_{(G)}$ and $\mathcal{M}^2_{(G)}$ is weaker than $\mathcal{H}^2_{(G)}$ for $a > a_{\rm crit}$. Thus, in order to prevent $\mathcal{H}$-accelerated instability, the initial value of the scale factor $a_{\rm ini}$ needs to be smaller than that critical value.

We also mention the growth of the perturbations around the bouncing point. Actually, it is found that the behavior is not quite different from the previous case with asymptotic Milne spacetime. It is reasonable because the effect of a cosmological constant is expected to be relatively weaker than those of higher-order curvature terms.

Oscillating solutions.—We examine the stabilities of the oscillating solutions, specifically, $\mathcal{O}^{[0;1]}$, $\mathcal{B}^{[1;1]}_{\rm O}$ for $a_{\rm min} \le a \le a_{\rm max}$, $\mathcal{O}^{[-1;1]}$, $\mathcal{O}^{[-1;-1]}$ and $\mathcal{O}^{[-1;-1]}_{\rm BC}$ for $a_{\rm min} \le a \le a_{\rm max}$. In this case, we also construct solutions whose squared effective masses are positive and dominate the $\mathcal{H}$-term within the possible ranges of the scale factor. A typical example is shown in Fig. 10. In our analysis, $\mathcal{M}^2$ of all perturbation modes are positive and greater than $\mathcal{H}^2$. It means that the solution is under the $\mathcal{M}^2$-dominated stability when $\mathcal{H} < 0$ and under the complete stability

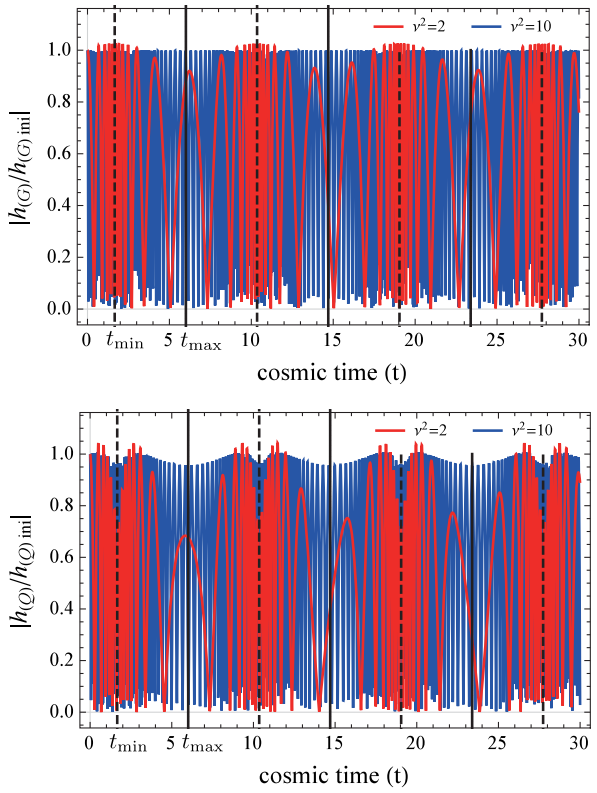

FIG. 11. The evolutions of perturbations in the oscillating solution $\mathcal{O}^{[-1;-1]}$ whose coupling constants are listed in Table II (x). In the top (bottom) figure, the evolution of tensor (scalar) perturbations are illustrated. The initial conditions are set to $a_{\mathrm{ini}} = (a_{\mathrm{min}} + a_{\mathrm{max}})/2 \approx 1.275$, and $\dot{h}_{(G)} = 0 = \dot{h}_{(Q)}$. The red and blue curves correspond to $\nu^2 = 2$ and 10, respectively. The dashed and solid black lines indicate the bouncing time and the recollapsing time, respectively. The first bouncing and recollapsing times are given by $t_{\mathrm{min}} \approx 1.660$ and $t_{\mathrm{max}} \approx 6.006$. The oscillating period of the scale factor is $T \approx 8.692$.

when $\mathcal{H} > 0$. It is remarkable that, in that case, the scalar perturbations with low ν^2 show $H\mathcal{H}_{(Q)} < 0$ around the bouncing point, which means that the scalar perturbations feel $\mathcal{H}$-friction slightly before the bounce and receive $\mathcal{H}$-acceleration slightly after the bounce.

Additionally, we show the dynamics of the tensor and scalar perturbations in the oscillating solution in Fig. 11. From these figures, the typical amplitudes of the perturbations are almost constant even if the Universe experiences a number of oscillations. Thus, we conclude the solution is stable with respect to the linear perturbations.

VI. SUMMARY AND DISCUSSIONS

We have investigated the stability of the singularity-free cosmological solutions based on the nonprojectable HL theory whose action is given by (2.4). Since our aim is to remedy the infrared behaviors of the singularity-free solutions in the projectable HL theory, we introduced only the single additional term Φ^2 which is expected to be dominant in infrared limit. It is remarkable that our gravitational action realizes the identical background solutions in FLRW spacetime based on the projectable HL theory with $\mathcal{C} = 0$. Therefore, the bouncing solutions and the oscillating solutions which are induced by the higher-order spatial derivative terms in the action are also found as in the projectable case.

By considering the quadratic action, we discuss the stability of the singularity-free solutions with respect to tensor and scalar perturbations. The stabilities can be estimated by the sign of the coefficients $\mathcal{F}$ and $\mathcal{G}$ showed in (4.27) and (4.33). $\mathcal{F} < 0$ corresponds to the ghost instability which is equivalent to a lack of the lowest energy state. The case with $\mathcal{G} < 0$ is known as the gradient instability which is interpreted as a unstable behavior due to the negative squared effective mass. However, it is possible to consider the case that the unstable behavior caused by $\mathcal{G} < 0$ is suppressed by the effect of background dynamics. As we showed in (5.1), the stability of the perturbations can be judged by the sign of the effective friction coefficients $\mathcal{H}$ and the effective squared masses $\mathcal{M}^2$, additionally the magnitude relationships between $\mathcal{H}^2$ and $|\mathcal{M}^2|$. Thus, we introduced five types of stabilities and instabilities (i) negative-$\mathcal{M}^2$ instability, (ii) $\mathcal{H}$-accelerated instability, (iii) $\mathcal{M}^2$-dominated stability, (iv) $\mathcal{H}$-suppressed stability, and (v) complete stability.

The novel feature of the singularity-free cosmological solutions in the nonprojectable HL theory is that we can find the bouncing solutions which satisfy the $\mathcal{M}^2$-dominated stability condition when $\mathcal{H} < 0$ and the complete stability condition when $\mathcal{H} > 0$. Such solutions cannot be constructed in the projectable HL theory, that is, the squared effective masses must be negative in infrared region.

We additionally investigate the stability of the oscillating solutions. The solution (x) we have shown in Sec. V B 3 is the stable solution which satisfy the $\mathcal{M}^2$-dominated stability condition when $\mathcal{H} < 0$ and the complete stability condition when $\mathcal{H} > 0$. In fact, the typical amplitudes of the perturbations stay almost constant.

However, we would like to indicate that it is not impossible to construct an oscillating solution whose typical perturbation amplitude is exponentially enhanced even if either $\mathcal{M}^2$-dominated stability condition or the complete stability condition is satisfied. That instability is caused by a resonance. Whether the resonance is induced or not can be investigated by the Hill's method [66] which is summarized in Appendix. We numerically show a example of the oscillating solution with resonance instability in Fig. 12 and the coupling constants of the solution is shown in Table IV. Note that this solution is satisfied both $\mathcal{M}^2$-stability condition and complete stability condition (see Fig. 13). In that case, certain modes of the tensor perturbation show unstable behavior. The Hill's method indicates that

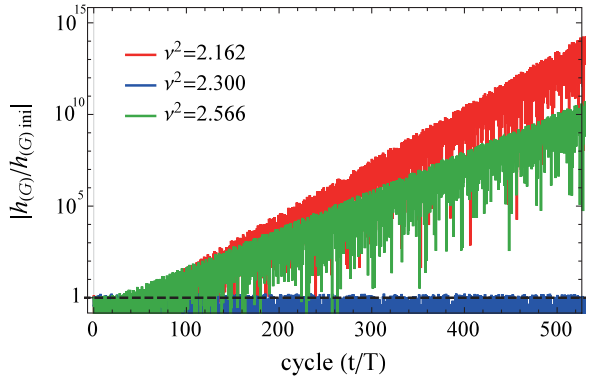

FIG. 12. The evolutions of the tensor perturbations in the oscillating solution where the coupling constants are listed in Table IV. The oscillating period of the scale factor is $T \approx 8.723$. The $\nu^2 = 2.162$ (red) and 2.556 (green) modes show the resonance, while the $\nu = 2.300$ (blue) mode is stable.

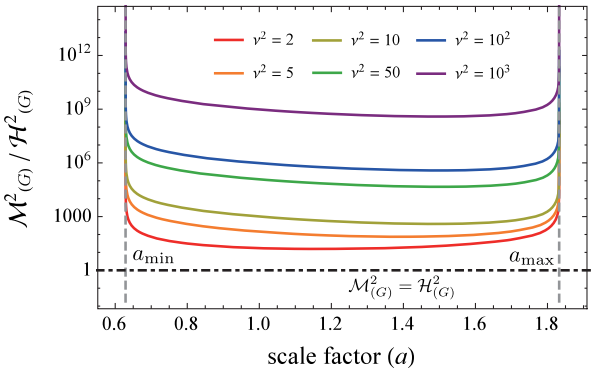

FIG. 13. The typical example of the ratios of the squared effective mass to the squared effective friction coefficient $\mathcal{M}^2_{(G)}/\mathcal{H}^2_{(G)}$ in the oscillating solution with resonance instability. The example solution is $\mathcal{O}^{[-1;-1]}$ whose values of coupling constants are given in Table IV. The red, orange, yellow, green, blue and purple curves indicate the evolutions with $\nu^2 = 2, 5, 10, 50, 10^2$ and 10^3, respectively ($\nu^2 = n^2 + 1$). The horizontal dot-dashed black lines indicate $\mathcal{M}^2_{(G)} = \mathcal{H}^2_{(G)}$. The vertical dashed gray lines indicate the maximum and minimum radii of the oscillation.

the degree of enhancement is characterized by $\epsilon_\pm$ defined in (A7). If $|\epsilon_\pm|$ exceeds 1, the amplitude of the corresponding perturbation mode exponentially grows. In fact, the solution includes certain tensor perturbation modes with $|\epsilon_\pm| > 1$ as we show in Fig. 14. It shows that even if all stability conditions we have discussed are satisfied, the oscillating solution is possibly unstable due to the resonance.

The oscillating solutions with resonance instability can be discovered if we set the coupling constant g_8 to be positive, however, relatively smaller than that of the stable solutions listed in Table II as far as our numerical analysis is concerned. One may notice that such a manipulation corresponds to consider the small effective squared mass. See (4.28) and (4.35), it is found that ultraviolet dominant terms $g_8\nu^6/a^6$ decrease. Thus, it is natural to consider that the heavy effective squared masses prevent the oscillating solution from the resonance instability. Actually, we can see from Fig. 14 that the degree of enhancement $|\epsilon_\pm|$ approaches unity as the perturbation mode ν^2 increases. We would like to stress that the resonance instability is mainly the problem in open FLRW spacetime. Since the perturbation mode ν^2 takes discrete number greater than or equal to eight in closed FLRW spacetime, the resonance instability is not quite problematic. In general terms, the positive heavy squared effective masses $\mathcal{M}^2$ is preferred to avoid the instabilities due to the background dynamics, i.e., $\mathcal{H}$-accelerated instability and the resonance instability. Thus, the higher-order curvature terms with $z = 3$ are significant to stabilize the spacetime as well as inducing the bounce.

We also mention the stability of singularity-free solutions based on the general covariant HL theory which is an alternative modification to remedy the behavior of scalar perturbation [67]. In this theory, the scalar propagating d.o.f. is eliminated by the additional fields, whereas the tensor perturbations are not modified. It is notable that the identical background solutions in FLRW spacetime to those of projectable and nonprojectable HL theory can be reproduced under certain conditions [68–70]. Therefore, the stability analyses we have performed are also valid in

TABLE IV. An example of the coupling constants for the oscillating solution with resonance.

Type	Λ	λ	g_2	g_3	g_4	g_5	g_6	g_7	g_8	ς	g_r	g_s	$a_{\min}$	$a_{\max}$
$\mathcal{O}^{[-1;-1]}$	-1	3	$\frac{1}{4}$	$-\frac{1}{2}$	0	$\frac{1}{20}$	$-\frac{1}{15}$	$-\frac{1}{5}$	$\frac{1}{5}$	$\frac{3}{2}$	$\frac{3}{2}$	1	0.629	1.832

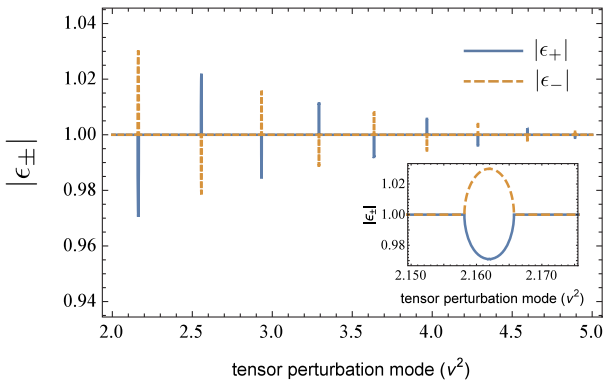

FIG. 14. The $\epsilon_\pm$ dependence on the tensor perturbation mode ν^2. The coupling constants are listed in Table IV. The solid blue line shows $|\epsilon_+|$, while the dashed orange line gives $|\epsilon_-|$. $|\epsilon_-|$ reaches a maximum ($\approx$1.030) at $\nu^2 \approx 2.162$ and $|\epsilon_+|$ reaches a maximum ($\approx$1.021) at $\nu^2 \approx 2.556$. This system causes the resonance around those modes.

the general covariant HL theory. For example, the background solutions with $g_3 = 0$ hold positive squared effective masses if the conditions we have explicitly shown in Sec. V B 1 are satisfied. Then, we can construct the stable singularity-free solutions only by examining $\mathcal{M}^2_{(\mathrm{G})}/H^2$.

The perturbative approach we have performed is based on a postulate. The effect of the backreaction can be ignored. In other words, the background dynamics are never affected by the perturbations. Of course, that assumption is not trivial. If the perturbation amplitudes are much enhanced, it is possible that the perturbation fields impinge on the background dynamics. Our numerical analysis shows that the typical amplitudes of the perturbations are enhanced around bouncing point. The degree of enhancement tends to be larger if $|\mathcal{M}^2|$ is small. Therefore, one may wonder how much the perturbation amplitude is allowed not to affect to the background dynamics. For certain perturbation mode, we can give an estimation. In fact, the tensor perturbations with $\nu^2 = 8$ in closed FLRW spacetime include the homogeneous modes, which corresponds the Bianchi-type IX spacetime whose anisotropy is small (in detail, see [48]). Thus it might be possible to estimate the effect of backreaction by considering more general background including inhomogeneity and anisotropy.

ACKNOWLEDGMENTS

The authors would like to thank K. Maeda and K. Aoki for their insightful comments and discussions. M. F. and S. S. are grateful to the Early Bird Program from Waseda Research Institute for Science and Engineering, Grant-in-Aid for Young Scientists. The work of S. M. was supported in part by Grants-in-Aid from the Scientific Research Fund of the Japan Society for the Promotion of Science (No. 18J11983).

APPENDIX: RESONANCE IN THE OSCILLATING SOLUTION

In the oscillating solutions, the perturbations feel periodical external forces, which may causes a resonance and the rapid growth of the perturbations. To clarify whether the resonance is induced or not, we examine the perturbation equations by adopting Hill's method. Since the procedures are completely the same between tensor and scalar perturbations, the subscripts which represent tensor and scalar modes are abbreviated in what follows.

To rewrite the equations into the Hill's form, we consider a field redefinition as

$$\hat{h} \coloneqq \sqrt{a^3\mathcal{F}}h. \tag{A1}$$

Then, the perturbation equations are transformed as

$$\frac{d^2\hat{h}}{dt^2} + \omega^2(t)\hat{h} = 0, \tag{A2}$$

with

$$\omega^2(t) \coloneqq \frac{1}{4}\left[\frac{\dot{\mathcal{F}}^2}{\mathcal{F}^2} - \frac{2(3H\dot{\mathcal{F}} + \ddot{\mathcal{F}})}{\mathcal{F}} - 9H^2 - 6\dot{H} + 4\mathcal{M}^2\right]. \tag{A3}$$

Since the effective squared angular frequency $\omega^2(t)$ is essentially a function which depends only on the scale factor, the oscillating period is expected to be the same as that of the scale factor. We further introduce the following equation in the matrix expression as

$$\frac{d}{dt}X(t) = \begin{pmatrix} 0 & 1 \\ -\omega^2(t) & 0 \end{pmatrix}X(t), \tag{A4}$$

$$X(t) \coloneqq \begin{pmatrix} \hat{h}(t) \\ \dot{\hat{h}}(t) \end{pmatrix}. \tag{A5}$$

Here, $\hat{h}(t)$ is an arbitrary perturbation function, and $X(t)$ is a real solution vector for the Hill equation (A2).

Let T be a period which is characterized by the effective squared angular momentum ω^2, then the evolution of X is expressed as

$$X(t+T) = \mathcal{A}X(t), \tag{A6}$$

where $\mathcal{A}$ is a 2×2 matrix which represents the time translation $t \to t+T$. Suppose $\{\epsilon_+, X_{\epsilon_+}\}$ and $\{\epsilon_-, X_{\epsilon_-}\}$ are two independent eigensystems of matrix $\mathcal{A}$, where $\epsilon_\pm$ are eigenvalues and $X_{\epsilon_\pm}$ are corresponding eigenvectors. Then, (A6) can be rewritten as some linear combination of the following relations:

$$X_{\epsilon_\pm}(t+T) = \epsilon_\pm X_{\epsilon_\pm}(t). \tag{A7}$$

Therefore, we find that both $|\epsilon_+| \le 1$ and $|\epsilon_-| \le 1$ are required to suppress the resonance of the perturbations.

To specify the explicit conditions for $|\epsilon_\pm| \le 1$, we introduce two independent complex vector X_1 and X_2 whose initial conditions are

$$X_1(0) = \begin{pmatrix} \hat{h}_1(0) \\ \dot{\hat{h}}_1(0) \end{pmatrix} = \begin{pmatrix} 1 \\ 0 \end{pmatrix}, \tag{A8}$$

$$X_2(0) = \begin{pmatrix} \hat{h}_2(0) \\ \dot{\hat{h}}_2(0) \end{pmatrix} = \begin{pmatrix} 0 \\ 1 \end{pmatrix}. \tag{A9}$$

Any solution vector can be constructed by the linear combination of X_1 and X_2. Substituting (A8) and (A9) into (A6), we find

$$\mathcal{A} = \begin{pmatrix} \hat{h}_1(T) & \hat{h}_2(T) \\ \dot{\hat{h}}_1(T) & \dot{\hat{h}}_2(T) \end{pmatrix}. \tag{A10}$$

Solving the Hill equation (A2) with these initial conditions, $\mathcal{A}$ can be estimated. The eigenvalues of $\mathcal{A}$ are obtained from the following equation.

$$\epsilon^2 - (\mathrm{tr}\mathcal{A})\epsilon + \det\mathcal{A} = 0. \tag{A11}$$

Since the Hill equation (A2) and the initial conditions (A8) and (A9) give $\det\mathcal{A} = 1$, the eigenvalues $\epsilon_\pm$ are given by

$$\epsilon_\pm = \frac{\mathrm{tr}\mathcal{A} \pm \sqrt{(\mathrm{tr}\mathcal{A})^2 - 4}}{2}. \tag{A12}$$

One can see that $|\mathrm{tr}\mathcal{A}| \leq 2$ is equivalent to $|\epsilon_\pm| = 1$. When $\epsilon_\pm$ is a complex number, the perturbations correspond to the real part of $X(t)$. For the case with $|\mathrm{tr}\mathcal{A}| > 2$, any one of $|\epsilon_\pm|$ is greater than unity. Thus, we conclude that if $|\mathrm{tr}\mathcal{A}| \leq 2$, the perturbation keeps oscillating forever without growing or decaying. On the other hand, the perturbation shows an exponential instability if $|\mathrm{tr}\mathcal{A}| > 2$.

[1] R. Penrose, Gravitational Collapse and Space-Time Singularities, Phys. Rev. Lett. **14**, 57 (1965); S. W. Hawking, The occurrence of singularities in cosmology. III. Causality and singularities, Proc. R. Soc. A **300**, 187 (1967); S. W. Hawking and R. Penrose, The singularities of gravitational collapse and cosmology, Proc. R. Soc. A **314**, 529 (1970); S. W. Hawking and G. F. R. Ellis, *The Large Scale Structure of Space-Time* (Cambridge University, Cambridge, England, 1973).

[2] A. Borde and A. Vilenkin, Eternal Inflation and the Initial Singularity, Phys. Rev. Lett. **72**, 3305 (1994); A. Borde, A. H. Guth, and A. Vilenkin, Inflationary Spacetimes are Incomplete in Past Directions, Phys. Rev. Lett. **90**, 151301 (2003).

[3] R. Brandenberger and P. Peter, Bouncing Cosmologies: Progress and Problems, Found. Phys. **47**, 797 (2017).

[4] J. Khoury, B. A. Ovrut, P. J. Steinhardt, and N. Turok, Ekpyrotic universe: Colliding branes and the origin of the hot big bang, Phys. Rev. D **64**, 123522 (2001); J. Khoury, B. A. Ovrut, N. Seiberg, P. J. Steinhardt, and N. Turok, From big crunch to big bang, Phys. Rev. D **65**, 086007 (2002).

[5] R. Brandenberger and C. Vafa, Superstrings in the early universe, Nucl. Phys. **B316**, 391 (1989); A. Nayeri, R. Brandenberger, and C. Vafa, Producing a Scale-Invariant Spectrum of Perturbations in a Hagedorn Phase of String Cosmology, Phys. Rev. Lett. **97**, 021302 (2006); R. Brandenberger, R. Costa, G. Franzmann, and A. Weltman, Point particle motion in double field theory and a singularity-free cosmological solution, Phys. Rev. D **97**, 063530 (2018).

[6] D. J. Mulryne, R. Tavakol, J. E. Lidsey, and G. F. R. Ellis, An emergent universe from a loop, Phys. Rev. D **71**, 123512 (2005).

[7] I. Agullo, A. Ashtekar, and W. Nelson, The pre-inflationary dynamics of loop quantum cosmology: Confronting quantum gravity with observations, Classical Quantum Gravity **30**, 085014 (2013).

[8] E. W. Ewing, Ekpyrotic loop quantum cosmology, J. Cosmol. Astropart. Phys. 08 (2013) 015.

[9] P. Creminelli, A. Nicolis, and E. Trincherini, Galilean genesis: An alternative to inflation, J. Cosmol. Astropart. Phys. 11 (2010) 021.

[10] D. A. Easson, I. Sawicki, and A. Vikman, G-Bounce, J. Cosmol. Astropart. Phys. 11 (2011) 021.

[11] S. Nishi and T. Kobayashi, Generalized galilean genesis, J. Cosmol. Astropart. Phys. 03 (2015) 057.

[12] T. Kobayashi, M. Yamaguchi, and J. Yokoyama, Galilean creation of the inflationary universe, J. Cosmol. Astropart. Phys. 07 (2015) 017.

[13] A. Ijjas, Space-time slicing in Horndeski theories and its implications for non-singular bouncing solutions, J. Cosmol. Astropart. Phys. 02 (2018) 007.

[14] D. A. Dobre, A. V. Frolov, J. T. G. Ghersi, S. Ramazanov, and A. Vikman, Unbraiding the bounce: Superluminality around the corner, J. Cosmol. Astropart. Phys. 03 (2018) 020.

[15] T. Biswas, E. Gerwick, T. Koivisto, and A. Mazumdar, Towards Singularity and Ghost-free Theories of Gravity, Phys. Rev. Lett. **108**, 031101 (2012); T. Biswas, A. S. Koshelev, A. Mazumdar, and S. Y. Vernov, Stable bounce and inflation in non-local higher derivative cosmology, J. Cosmol. Astropart. Phys. 08 (2012) 024; Á. de la Cruz-Dombriz, F. J. M. Torralba, and A. Mazumdar, Non-singular and ghost-free infinite derivative gravity with torsion, arXiv:1812.04037.

[16] T. Kobayashi, Generic instabilities of non-singular cosmologies in Horndeski theory: A no-go theorem, Phys. Rev. D **94**, 043511 (2016).

[17] S. Akama and T. Kobayashi, Generalized multi-Galileons, covariantized new terms, and the no-go theorem for non-singular cosmologies, Phys. Rev. D **95**, 064011 (2017).

[18] S. Akama and T. Kobayashi, General theory of cosmological perturbations in open and closed universes from the Horndeski action, arXiv:1810.01863.

[19] R. Kolevatov and S. Mironov, Cosmological bounces and Lorentzian wormholes in Galileon theories with an extra scalar field, Phys. Rev. D **94**, 123516 (2016).

[20] G. W. Horndeski, Second-order scalar-tensor field equations in a four-dimensional space, Int. J. Theor. Phys. **10**, 363 (1974); T. Kobayashi, M. Yamaguchi, and J. Yokoyama, Generalized G-inflation: Inflation with the most general second-order field equations, Prog. Theor. Phys. **126**, 511 (2011).

[21] A. Ijjas and P. J. Steinhardt, Classically Stable Nonsingular Cosmological Bounces, Phys. Rev. Lett. **117**, 121304 (2016); A. Ijjas and P. J. Steinhardt, Fully stable cosmological solutions with a non-singular classical bounce, Phys. Lett. B **764**, 289 (2017).

[22] Y. Cai, Y. Wan, H-G. Li, T. Qiu, and Y-S. Piao, The effective field theory of nonsingular cosmology, J. High Energy Phys. 01 (2017) 090; Y. Cai, Y. Wan, H.-G. Li, T. Qiu, and

Y.-S. Piao, The effective field theory of nonsingular cosmology: II, Eur. Phys. J. C **77**, 369 (2017).
[23] P. Creminelli, D. Pirtskhalava, L. Santoni, and E. Trincherini, Stability of geodesically complete cosmologies, J. Cosmol. Astropart. Phys. 11 (2016) 047.
[24] S. Banerjee and E. N. Saridakis, Bounce and cyclic cosmology in weakly broken galileon theories, Phys. Rev. D **95**, 063523 (2017).
[25] R. Kolevatov, S. Mironov, N. Sukhov, and V. Volkova, Cosmological bounce and genesis beyond Horndeski, J. Cosmol. Astropart. Phys. 08 (2017) 038.
[26] P. Hořava, Quantum gravity at a Lifshitz point, Phys. Rev. D **79**, 084008 (2009).
[27] A. Wang, Hořava gravity at a Lifshitz point: A progress report, Int. J. Mod. Phys. D **26**, 1730014 (2017).
[28] T. Fujimori, T. Inami, K. Izumi, and T. Kitamura, Power-counting and renormalizability in Lifshitz scalar theory, Phys. Rev. D **91**, 125007 (2015); T. Fujimori, T. Inami, K. Izumi, and T. Kitamura, Tree-level unitarity and renormalizability in Lifshitz scalar theory, Prog. Theor. Exp. Phys. **2016**, 013B08 (2016).
[29] A. O. Barvinsky, D. Blas, M. Herrero-Valea, S. M. Sibiryakov, and C. F. Steinwachs, Renormalization of Horava gravity, Phys. Rev. D **93**, 064022 (2016).
[30] S. Mukhoyama, Hořava-Lifshitz cosmology: A review, Classical Quantum Gravity **27**, 223101 (2010).
[31] S. Mukhoyama, Scale-invariant cosmological perturbations from Hořava-Lifshitz gravity without inflation, J. Cosmol. Astropart. Phys. 90 (2009) 001.
[32] R. Cai, B. Hu, and H. Zhang, Dynamical scalar degree of freedom in Horava-Lifshitz gravity, Phys. Rev. D **80**, 041501 (2009).
[33] T. Kobayashi, Y. Urakawa, and M. Yamaguchi, Large scale evolution of the curvature perturbation in Horava-Lifshitz cosmology, J. Cosmol. Astropart. Phys. 11 (2009) 015.
[34] A. Wang, D. Wands, and R. Maartens, Scalar field perturbations in Hořava-Lifshitz cosmology, J. Cosmol. Astropart. Phys. 03 (2010) 013; A. Wang, Vector and tensor perturbations in Horava-Lifshitz cosmology, Phys. Rev. D **82**, 124063 (2010).
[35] K. Izumi, T. Kobayashi, and S. Mukohyama, Non-Gaussianity from Lifshitz scalar, J. Cosmol. Astropart. Phys. 10 (2010) 031.
[36] T. Takahashi and J. Soda, Chiral Primordial Gravitational Waves from a Lifshitz Point, Phys. Rev. Lett. **102**, 231301 (2009).
[37] A. E. Gümrükçüoğlu, M. Saravani, and T. P. Sotiriou, Hořava gravity after GW170817, Phys. Rev. D **97**, 024032 (2018).
[38] S. Mukohyama, K. Nakayama, F. Takahashi, and S. Yokoyama, Phenomenological aspects of Hořava-Lifshitz cosmology, Phys. Lett. B **679**, 6 (2009).
[39] S. Mukohyama, Dark matter as integration constant in Horava-Lifshitz gravity, Phys. Rev. D **80**, 064005 (2009).
[40] A. Wang and Y. Wu, Thermodynamics and classification of cosmological models in the Horava-Lifshitz theory of gravity, J. Cosmol. Astropart. Phys. 07 (2009) 012.
[41] Y. Q. Huang, A. Wang, and Q. Wu, Stability of the de Sitter spacetime in Horava-Lifshitz theory, Mod. Phys. Lett. A **25**, 2267 (2010); A. Wang and Q. Wu, Stability of spin-0 graviton and strong coupling in Horava-Lifshitz theory of gravity, Phys. Rev. D **83**, 044025 (2011).
[42] G. Calcagni, Cosmology of the Lifshitz universe, J. High Energy Phys. 09 (2009) 112.
[43] E. Kiritsis and G. Kofinas, Horava-Lifshitz Cosmology, Nucl. Phys. **B821**, 467 (2009).
[44] R. H. Brandenberger, Matter bounce in Horava-Lifshitz cosmology, Phys. Rev. D **80**, 043516 (2009).
[45] Y. F. Cai and E. N. Saridakis, Non-singular cosmology in a model of non-relativistic gravity, J. Cosmol. Astropart. Phys. 10 (2009) 020.
[46] K. Maeda, Y. Misonoh, and T. Kobayashi, Oscillating universe in Horava-Lifshitz gravity, Phys. Rev. D **82**, 064024 (2010).
[47] Y. Misonoh, K. Maeda, and T. Kobayashi, Oscillating Bianchi IX universe in Horava-Lifshitz gravity, Phys. Rev. **D84**, 064030 (2011).
[48] Y. Misonoh, M. Fukushima, and S. Miyashita, Stability of singularity-free cosmological solutions in Hořava-Lifshitz gravity, Phys. Rev. D **95**, 044044 (2017).
[49] C. Charmousis, G. Niz, A. Padilla, and P. M. Saffin, Strong coupling in Hořava gravity, J. High Energy Phys. 08 (2009) 070.
[50] M. Li and Y. Pang, A trouble with Hořava-Lifshitz gravity, J. High Energy Phys. 08 (2009) 015.
[51] D. Blas, O. Pujolas, and S. Sibiryakov, On the extra mode and inconsistency of Hořava gravity, J. High Energy Phys. 10 (2009) 029.
[52] K. Koyama and F. Arroja, Pathological behaviour of the scalar graviton in Hořava-Lifshitz gravity, J. High Energy Phys. 03 (2010) 061.
[53] D. Blas, O. Pujolas, and S. Sibiryakov, Consistent Extension of Hořava Gravity, Phys. Rev. Lett. **104**, 181302 (2010); Strong coupling in extended Hořava-Lifshitz gravity, Phys. Lett. B **685**, 197 (2010); Comment on Strong coupling in extended Hořava-Lifshitz gravity, Phys. Lett. B **688**, 350 (2010); Models of non-relativistic quantum gravity: The good, the bad and the healthy, J. High Energy Phys. 04 (2011) 018.
[54] T. Kobayashi, Y. Urakawa, and M. Yamaguchi, Cosmological perturbations in a healthy extension of Hořava gravity, J. Cosmol. Astropart. Phys. 04 (2010) 025.
[55] R. G. Cai, B. Hu, and H. B. Zhang, Scalar graviton in the healthy extension of Hořava-Lifshitz theory, Phys. Rev. D **83**, 084009 (2011).
[56] T. Jacobson, Extended Hořava gravity and Einstein-aether theory, Phys. Rev. D **81**, 101502 (2010); Erratum, Phys. Rev. D **82**, 129901 (2010).
[57] D. Blas and S. Sibiryakov, Hořava gravity versus thermodynamics: The black hole case, Phys. Rev. D **84**, 124043 (2011).
[58] E. Barausse, T. Jacobson, and T. P. Sotiriou, Black holes in Einstein-aether and Hořava-Lifshitz gravity, Phys. Rev. D **83**, 124043 (2011).
[59] P. Berglund, J. Bhattacharyya, and D. Mattingly, Mechanics of universal horizons, Phys. Rev. D **85**, 124019 (2012).
[60] K. Lin, E. Abdalla, R. G. Cai, and A. Wang, Universal horizons and black holes in gravitational theories with broken Lorentz symmetry, Int. J. Mod. Phys. D **23**, 1443004 (2014).

[61] K. Lin, V. H. Satheeshkumar, and A. Wang, Static and rotating universal horizons and black holes in gravitational theories with broken Lorentz invariance, Phys. Rev. D **93**, 124025 (2016).

[62] Y. Misonoh and K. Maeda, Black holes and thunderbolt singularities with Lifshitz scaling terms, Phys. Rev. D **92**, 084049 (2015).

[63] E. G. M. Ferreira and R. Brandenberger, Trans-Planckian problem in the healthy extension of Hořava-Lifshitz gravity, Phys. Rev. D **86**, 043514 (2012).

[64] T. P. Sotiriou, M. Visser, and S. Weinfurtner, Phenomenologically Viable Lorentz-Violating Quantum Gravity, Phys. Rev. Lett. **102**, 251601 (2009); Quantum gravity without Lorentz invariance, J. High Energy Phys. 10 (2009) 033.

[65] B. P. Abbott *et al.* (LIGO Scientific and Virgo Collaborations), GW170817: Observation of Gravitational Waves from a Binary Neutron Star Inspiral, Phys. Rev. Lett. **119**, 161101 (2017); B. P. Abbott *et al.* (LIGO Scientific and Virgo Collaborations, Fermi Gamma-Ray Burst Monitor and INTEGRAL), Gravitational waves and gamma-rays from a binary neutron star merger: GW170817 and GRB 170817A, Astrophys. J. **848**, L13 (2017).

[66] G. W. Hill, On the part of the motion of the lunar perigee which is a function of the mean motions of the sun and moon, Acta Math. **8**, 1 (1886).

[67] P. Horava and C. M. Melby-Thompson, General covariance in quantum gravity at a Lifshitz point, Phys. Rev. D **82**, 064027 (2010).

[68] A. Wang and Y. Wu, Cosmology in nonrelativistic general covariant theory of gravity, Phys. Rev. D **83**, 044031 (2011).

[69] T. Zhu, Q. Wu, A. Wang, and F. Shu, U(1) symmetry and elimination of spin-0 gravitons in Horava-Lifshitz gravity without the projectability condition, Phys. Rev. D **84**, 101502 (2011).

[70] T. Zhu, F.-W. Shu, Q. Wu, and A. Wang, General covariant Horava-Lifshitz gravity without projectability condition and its applications to cosmology, Phys. Rev. D **85**, 044053 (2012).